

UNCLASSIFIED

AD NUMBER	
AD063985	
CLASSIFICATION CHANGES	
TO:	UNCLASSIFIED
FROM:	CONFIDENTIAL
LIMITATION CHANGES	
TO: Approved for public release; distribution is unlimited.	
FROM: Distribution authorized to U.S. Gov't. agencies and their contractors; Administrative/Operational Use; 06 JUN 1955. Other requests shall be referred to Naval Proving Ground, Dahlgren, VA.	
AUTHORITY	
30 Jun 1967, DoDD 5200.10; USNSWC ltr, 5 Mar 1975	

THIS PAGE IS UNCLASSIFIED

THIS REPORT HAS BEEN DELIMITED
AND CLEARED FOR PUBLIC RELEASE
UNDER DOD DIRECTIVE 5200.20 AND
NO RESTRICTIONS ARE IMPOSED UPON
ITS USE AND DISCLOSURE.

DISTRIBUTION STATEMENT A

APPROVED FOR PUBLIC RELEASE;
DISTRIBUTION UNLIMITED.

UNCLASSIFIED

AD _____

*Reproduced
by the*

ARMED SERVICES TECHNICAL INFORMATION AGENCY
ARLINGTON HALL STATION
ARLINGTON 12, VIRGINIA



DOWNGRADED AT 3 YEAR INTERVALS:
DECLASSIFIED AFTER 12 YEARS
DOD DIR 5200.10

UNCLASSIFIED

AD 63985

Armed Services Technical Information Agency

Reproduced by
DOCUMENT SERVICE CENTER
KNOTT BUILDING, DAYTON, 2, OHIO

Because of our limited supply, you are requested to
RETURN THIS COPY WHEN IT HAS SERVED YOUR PURPOSE
so that it may be made available to other requesters.
Your cooperation will be appreciated.

NOTICE: WHEN GOVERNMENT OR OTHER DRAWINGS, SPECIFICATIONS OR OTHER DATA ARE USED FOR ANY PURPOSE OTHER THAN IN CONNECTION WITH A DEFINITELY RELATED GOVERNMENT PROCUREMENT OPERATION, THE U. S. GOVERNMENT THEREBY INCURS NO RESPONSIBILITY, NOR ANY OBLIGATION WHATSOEVER; AND THE FACT THAT THE GOVERNMENT MAY HAVE FORMULATED, FURNISHED, OR IN ANY WAY SUPPLIED THE SAID DRAWINGS, SPECIFICATIONS, OR OTHER DATA IS NOT TO BE REGARDED BY IMPLICATION OR OTHERWISE AS IN ANY MANNER LICENSING THE HOLDER OR ANY OTHER PERSON OR CORPORATION, OR CONVEYING ANY RIGHTS OR PERMISSION TO MANUFACTURE, USE OR SELL ANY PATENTED INVENTION THAT MAY IN ANY WAY BE RELATED THERETO.

~~CONFIDENTIAL~~
NPG Report No. 1211

FC

63985

THE WINDSHIELD EFFECT, THE HOOD EFFECT, AND THE CAP EFFECT



U. S. NAVAL PROVING GROUND
DAHLGREN, VIRGINIA

Copy No. 11

Date 6 June 1955

~~CONFIDENTIAL~~
55AA

22473

JUN 30 1955

~~CONFIDENTIAL~~
U. S. NAVAL PROVING GROUND
DAHLGREN, VIRGINIA


The Windshield Effect, The Hood Effect, and The Cap Effect

By

A. V. Hershey
Computation and Ballistics Department

NPG REPORT NO. 1211
Task Assignment No. K-11011-1
Date: 6 June 1955

APPROVED: J. F. BYRNE
Captain, USN
Commander, Naval Proving Ground


E. A. RUCKNER
Captain, USN
Ordnance Officer
By direction

~~CONFIDENTIAL~~
55A A

22473

CONTENTS

	<u>Page</u>
Abstract	ii
Foreword	iii
Introduction	1
The Ballistic Parameters	2
The Geometry of an Ogive	2
The Motion of the Body	5
The Windshield Effect	7
The Dynamics of the Windshield	7
Performance on Normal Impact	8
Performance on Oblique Impact	9
Static Tests	9
Dynamic Tests	10
The Hood Effect	11
Dynamics of the Hood	11
Dynamic Tests	15
The Cap Effect	16
The Dynamics of the Cap	16
Ballistic Tests	18
Appendices:	
A and B. Indefinite Integrals for Ogives	19
C. Tables of Values	21
D. Tables of Data	30
E. List of Symbols	62
F. Bibliography	65
G. Set of Figures - Schematic Diagrams and Photographs	1-11
H. Distribution	67

ABSTRACT

The windshield and the hood of a common projectile are demolished during the early part of an impact, and disturb the motion of the body. The force and torque on the body arise from plastic and dynamic stresses in the windshield and hood. A theory is developed for the limiting case of low velocity where the plastic stress predominates, and a theory is developed for the limiting case of high velocity where the dynamic stress predominates. The limiting theories are blended for plates of intermediate thickness by the aid of the ballistic data for common projectiles. A study is made of the multiplicity of fractures in a hood whose fragments were recovered after impact. The cap of an AP projectile is shattered on impact against a thick plate, and the fragments of the cap disturb the flow and fracture of the armor plate. The effect on the energy for penetration has been inferred from the ballistic data for AP projectiles.

FOREWORD

The material in this report has been prepared since World War II in connection with a study of the mechanism of penetration of plate by projectiles. The report is one of a series of reports. Five of the reports were published at the end of the war, and it was originally planned that nine reports would be submitted altogether. The remaining four reports were held up pending a revaluation of the ballistic data, inasmuch as there was an opportunity to obtain a few additional tests of special interest at the end of the war. As a result of these tests, the number of reports has been increased to eleven. The six remaining reports are now to be published, but with a minimum expenditure of additional effort in order to bring forth the existing material. The analysis has probably been carried as far as it should be carried without the aid of a modern calculator such as the Aiken Dahlgren Electronic Calculator. The press of urgent work has thus far prevented allocation of any ADEC time to this work.

The titles of the full set of eleven reports are as follows:

- (1) ANALYTICAL SUMMARY. PART I. THE PHYSICAL PROPERTIES OF STS UNDER TRIAXIAL STRESS. NPG Report No. 6-46

Object: To summarize the available data on the physical properties of Class B Armor and STS under triaxial stress.

- (2) ANALYTICAL SUMMARY. PART II. ELASTIC AND PLASTIC UNDULATIONS IN ARMOR PLATE. NPG Report No. 7-46

Object: To analyse the propagation of undulations in armor plate; to summarize previous analytical work and to add new analytical work where required in order to complete the theory for ballistic applications.

- (3) ANALYTICAL SUMMARY. PART III. PLASTIC FLOW IN ARMOR PLATE. NPG Report No. 864

Object: To analyse the plastic flow in armor plate adjacent to the point of impact by a projectile.

- (4) ANALYTICAL SUMMARY. PART IV. THE THEORY OF ARMOR PENETRATION. NPG Report No. 9-46

Object: To summarize the theory of armor penetration in its present state of development, and to develop theoretical functions which can be used as a guide in the interpretation of ballistic data.

- (5) ANALYTICAL SUMMARY. PART V. PLASTIC FLOW IN BARS AND SHELLS. NPG Report No. 954

Object: To analyse the plastic flow in cylindrical bars and shells during impact against an unyielding plate.

- (6) ANALYTICAL SUMMARY. PART VI. THE THEORY OF PROJECTILE RICOCHET. NPG Report No. 1041

Object: To analyse the dynamics of projectiles during oblique impact, and to develop theoretical functions which can be used as a guide in the interpretation of ballistic data.

- (7) BALLISTIC SUMMARY. PART I. THE DEPENDENCE OF LIMIT VELOCITY ON PLATE THICKNESS AND OBLIQUITY AT LOW OBLIQUITY. NPG Report No. 2-46

Object: To compare the results of ballistic test with the prediction of existing formulae, and with the results of theoretical analysis; to find the mathematical functions which best represent fundamental relationship between limit velocity, plate thickness, and obliquity at low obliquity.

- (8) BALLISTIC SUMMARY. PART II. THE SCALE EFFECT AND THE OGIVE EFFECT. NPG Report No. 4-46

Object: To determine the effect of scale on ballistic performance, and to correlate the projectile nose shape with the results of ballistic test.

- (9) BALLISTIC SUMMARY. PART III. THE WINDSHIELD EFFECT, THE HOOD EFFECT, AND THE CAP EFFECT. NPG Report No. 1211

Object: To determine the effect of windshields and hoods or caps on ballistic performance.

- (10) BALLISTIC SUMMARY. PART IV. THE DEPENDENCE OF LIMIT VELOCITY ON PLATE THICKNESS AND OBLIQUITY AT HIGH OBLIQUITY. NPG Report No. 1125

Object: To compare the results of ballistic test with the results of theoretical analysis; to find mathematical functions which best represent the fundamental relationship between limit velocity, plate thickness, and obliquity at high obliquity.

- (11) BALLISTIC SUMMARY. PART V. THE CONSTRUCTION OF PLATE PENETRATION CHARTS OR TABLES. NPG Report No. 1120

Object: To summarize the results of analysis in the form of standard charts or tables.

This is the 19th partial report on the Foundational Research Program of the Naval Proving Ground; the 6th partial report on The Investigation of the Mechanics of Armor Penetration; and the final report on Ballistic Summary Part III - The Windshield Effect, the Hood Effect, and the Cap Effect. This project was originally authorized by BUORD ltr NP9/A9(Re3) of 9 January 1943, was later charged to Task Assignment NPG-41-Re3a-118-1, and is currently charged to the Foundational Research Program of the Naval Proving Ground.

The project work reported herein was conducted to determine the effect of windshields and hoods or caps on ballistic performance.

The computations for this report were performed by:

V. L. Nichols and J. M. Foster
Mathematical Physics Branch
Computation and Ballistics Department

This report was reviewed by:

N. A. M. Riffolt
Director of Research

INTRODUCTION

Service projectiles differ from monobloc projectiles by having a windshield and hood or cap which are attached to the nose of the projectile.

The windshield gives better flight characteristics to the projectile, while the hood holds the windshield in place. The windshield and hood are thin hollow shells and are made of soft materials so that they will not interfere greatly with the terminal ballistics of the projectile. The hood is secured to the nose of the projectile with soft solder. The windshield is usually welded to a threaded ring, and the threaded ring is screwed onto the hood. At the beginning of the penetration cycle, the hood and windshield are trapped between the plate and the body of the projectile.

The windshield is demolished by the plate and diverts a small fraction of the impact energy from the penetration. The windshield applies a force and torque to the body of the projectile which gives the body small increments in obliquity, yaw, and rate of yaw. The body requires more energy for penetration than a monobloc projectile.

The hood remains undeformed during impact against very thin plates, but flows plastically and fractures during impact against thick plates. The stress in the hood is partly plastic and partly dynamic. The plastic stress predominates at low striking velocity while the dynamic stress predominates at high striking velocity.

The cap absorbs the transient stress at the instant of impact and protects the body of the projectile from deformation. The cap is a thick cup of hard material. The cap remains undeformed during impact against thin plates, but breaks up during impact against thick plates.

The effect of the windshield and hood or cap on the limit velocity for perforation is revealed by a series of comparative ballistic tests on complete projectiles and on projectiles with the windshield and hood or cap removed. The number of such tests which have been completed to date are sufficient to outline the general trends of the windshield effect and hood or cap effect. Some of the ballistic data have been released in previous reports, references (4) to (9), but are summarized in Tables XIV and XV in the present report.

Semiquantitative theories for the windshield effect and the hood effect have been completed for the 6" Comm Mk 27-7 projectile, and the details of the theories are summarized in the present report. The theories have been guided by special static and dynamic tests of a fundamental nature. The theories are used to supplement the ballistic data in those ranges of impact conditions where the ballistic data are lacking.

THE BALLISTIC PARAMETERS

The results of ballistic test may conveniently be summarized in terms of ballistic parameters. The plate penetration coefficient $F(e/d, \theta)$ and the limit energy function $U(e/d, \theta)$ are defined in terms of the projectile mass m , the projectile diameter d , the plate thickness e , the obliquity θ , and the limit velocity v_L by the equations

$$F\left(\frac{e}{d}, \theta\right) = \frac{m^{1/2} v_L \cos \theta}{e^{1/2} d}$$

$$U\left(\frac{e}{d}, \theta\right) = \left(\frac{e}{d}\right) F^2\left(\frac{e}{d}, \theta\right) = \frac{m v_L^2 \cos^2 \theta}{d^3}$$

The whole mass of the projectile is used in the functions. The projectile mass is expressed in (lb), the projectile diameter is expressed in (ft), the plate thickness in (ft), and the limit velocity in (ft)/(sec).

The effects of windshields and hoods or caps are best represented by the increment ΔF between the plate penetration coefficient for the complete projectile and the plate penetration coefficient for a monobloc projectile.

THE GEOMETRY OF AN OGIVE

The body, the hood or cap, and the windshield have surfaces which are parts of ogival contours. Let i, j, k be three orthogonal unit vectors, among which the vector i is parallel to the plate and perpendicular to the axis of the projectile, the vector j is parallel to the plate but perpendicular to the vector i , and the vector k is perpendicular to the plate. The vector k is pointed toward the back of the plate. The axis of the projectile is inclined at the angle χ to the vector k . A point on the ogive may be defined in terms of cylindrical polar coordinates r, ϕ, z , which have the axis of the projectile for a polar axis. The coordinate r is the distance of the point from the axis of the projectile, the coordinate ϕ is a polar angle which is referred to the axis i , and the coordinate z is the distance of the point from a plane which is normal to the polar axis through the tip of the ogive.

A plane parallel to the plate intercepts the ogive in an oval curve. Let x, y be the Cartesian coordinates of the curve of intersection. The

coordinates x, y are given by the equations

$$x = r \cos \phi \qquad y = -p \tan \chi + r \frac{\sin \phi}{\cos \chi} \qquad (1)$$

in which p is the penetration of the tip into the plane of intersection.

In the case of an ogive with ogival radius R , the equation of the ogive is

$$(R - a + r)^2 + \left(b - \frac{p}{\cos \chi} + r \sin \phi \tan \chi\right)^2 = R^2 \qquad (2)$$

in which a is the maximum value of r , or the value of r at the circle where the ogive is tangent to a coaxial cylinder, and b is the distance from the circle of tangency to the tip of the ogive. The equation of the ogive may be solved with the aid of the quadratic formula to give r as a function of ϕ, χ . The radius r is also given by the equation

$$r = - (R - a) + \sqrt{R^2 - (b - z)^2} \qquad (3)$$

Let the unit vector n be normal to the nose contour at a point on the curve of intersection. The Cartesian components of n are given by the expressions

$$\begin{aligned} & + \frac{1}{R}(R - a + r) \cos \phi & i \\ & + \frac{1}{R}(R - a + r) \sin \phi \cos \chi + \frac{1}{R}\left(b - \frac{p}{\cos \chi} + r \sin \phi \tan \chi\right) \sin \chi & j \\ & - \frac{1}{R}(R - a + r) \sin \phi \sin \chi + \frac{1}{R}\left(b - \frac{p}{\cos \chi} + r \sin \phi \tan \chi\right) \cos \chi & k \end{aligned}$$

Let the unit vector t be tangent to the nose contour at the point on the curve of intersection, and let t be coplanar with the axis of the

projectile. The Cartesian components of t are given by the expressions

$$\begin{aligned}
 & + \frac{1}{R} \left(b - \frac{p}{\cos \chi} + r \sin \phi \tan \chi \right) \cos \phi & i \\
 & - \frac{1}{R} (R - a + r) \sin \chi & + \frac{1}{R} \left(b - \frac{p}{\cos \chi} + r \sin \phi \tan \chi \right) \sin \phi \cos \chi & j \\
 & - \frac{1}{R} (R - a + r) \cos \chi & - \frac{1}{R} \left(b - \frac{p}{\cos \chi} + r \sin \phi \tan \chi \right) \sin \phi \sin \chi & k
 \end{aligned}$$

That surface area s of the ogive which extends from any plane cross section to the tip of the ogive is given by the equation

$$s = 2\pi \int r \sqrt{1 + \left(\frac{dr}{dz}\right)^2} dz \quad (4)$$

The center of gravity of this surface is located at a distance from the circle of tangency which is given by the expression

$$\frac{1}{s} \int (b - z) ds$$

and the square of the radius of gyration of the surface, referred to an axis which is normal to the axis of symmetry at the bourrelet, is given by the expression

$$\frac{1}{s} \int \left\{ (b - z)^2 + \frac{1}{2} r^2 \right\} ds$$

The indefinite integrals which are required for the evaluation of these expressions are given in Appendix A.

That volume τ of the ogive which extends from any plane cross section to the tip of the ogive is given by the equation

$$\tau = \pi \int r^2 dz \quad (5)$$

The center of mass of this volume is located at a distance from the circle of tangency which is given by the expression

$$\frac{\int (b - z) r^2 dz}{\int r^2 dz}$$

and the square of the radius of gyration of the surface, referred to an axis which is normal to the axis of symmetry at the bourrelet, is given by the expression

$$\frac{\int \left\{ (b - z)^2 + \frac{1}{4} r^2 \right\} r^2 dz}{\int r^2 dz}$$

The indefinite integrals which are required for the evaluation of these expressions are given in Appendix B.

THE MOTION OF THE BODY

The windshield and the hood apply to the body a longitudinal force f_1 along the axis of the projectile, a transverse force f_2 normal to the axis, and a torque L about a transverse axis. The forces and torque are applied to the body at the beginning of the impact when the velocity of the projectile is greatest.

The longitudinal force f_1 on the body changes the kinetic energy of the body by an increment Δw which is given approximately by the equation

$$\Delta w = + \int_0^z f_1 dz \quad (6)$$

in which z is the displacement of the body along its line of flight. The transverse force f_2 on the body deflects the line of flight through an obliquity $\Delta\theta$, which is given by the equation

$$\Delta\theta = \frac{1}{m_0 v_s^2} \int_0^z f_2 dz \quad (7)$$

in which m_0 is the mass of the body and v_s is the striking velocity. The torque L gives the body an increment in rate of yaw $\Delta\dot{\chi}$, which is given by the equation

$$\Delta\dot{\chi} = - \frac{1}{C v_s} \int_0^z L dz \quad (8)$$

in which C is the transverse moment of inertia of the body. The torque rotates the body through a small angle of yaw $\Delta\chi$, which is given by the equation

$$\Delta\chi = - \frac{1}{C v_s} \left\{ z \int_0^z L dz - \int_0^z z L dz \right\} \quad (9)$$

Insofar as the windshield and hood have no direct influence on the mode of fracture of the plate, the windshield and hood contribute, to the plate penetration coefficient F , an increment ΔF , which is required to put the body through the plate. The increment ΔF is given to a first order approximation by the equation

$$\frac{\Delta F}{F} = \frac{1}{2} \frac{(m_1 + m_2)}{m_0} - \frac{\Delta w}{m_0 v_L^2} + (\tan \theta + \frac{1}{F} \frac{\partial F}{\partial \theta}) \Delta \theta + \frac{1}{F} \frac{\partial F}{\partial \chi} \Delta \chi + \frac{1}{F} \frac{\partial F}{\partial \dot{\chi}} \Delta \dot{\chi} \quad (10)$$

in which m_1 and m_2 are the masses of the windshield and hood, and the function F is assumed to be a function of $\theta, \chi, \dot{\chi}$. The sum

$$\frac{\partial F}{\partial \theta} + \frac{\partial F}{\partial \chi}$$

for a monobloc projectile may be derived from the conventional plate penetration data for which $\theta = \chi$. The effect of yaw and of rate of yaw have not been adequately determined for oblique impact, although experimental data might be obtained with long-travel rocket launchers. Theoretical data in reference (12) have therefore been interpolated.*

In the limiting case of a thin plate, the equation for ΔF may be condensed to the equation

$$\frac{\Delta F}{F} = \frac{1}{2} \frac{(m_1 + m_2)}{m_0} + \frac{1}{U} (\Theta_1 + \Theta_2)$$

in which U is the limit energy function and Θ_1, Θ_2 are functions of θ . In the limiting case of a thick plate, the ratio $\Delta F/F$ is a function of θ only.

* The derivatives of the function F in the present report are identified with the derivatives of a function h'_0 in reference (12) by the aid of the equations

$$\frac{1}{F} \frac{\partial F}{\partial \chi} = \frac{1}{h'_0} \frac{\partial h'_0}{\partial \chi_0}$$

and

$$\frac{v_L \cos \theta}{d} \frac{1}{F} \frac{\partial F}{\partial \dot{\chi}} = \frac{\partial h'_0}{\partial \dot{\chi}_0}$$

THE WINDSHIELD EFFECTDynamics of the windshield

When the forces and moments in the windshield are small, the windshield is in an elastic state, and stress in the windshield is propagated with the velocity of sound, which is much greater than the velocity of the projectile. The motion of the windshield is then given by the dynamics of rigid bodies. Since the windshield is much lighter than the rest of the projectile, it tends to remain at equilibrium under the forces applied to it as long as it remains rigidly attached to the body of the projectile.

The threshold of elastic instability in the windshield would be reached when the force on the windshield has a constant limiting value which is a function of the thickness of the windshield but is independent of the radius¹¹. The critical stress for elastic instability is much greater than the yield stress, and the windshield therefore yields before it buckles.

The longitudinal force f_1 and the transverse force f_2 are transmitted undiminished along the windshield at equilibrium. The cross section of the windshield increases from tip to base. The stress therefore decreases from tip to base and reaches the yield point at a short distance from the face of the plate. There is a narrow plastic zone next to the plate where the windshield flattens out on the plate. If the surface of contact between the plate and windshield is frictionless, the plate applies to the windshield a force which is normal to the surface of contact.

It is assumed in the present analysis that the force on the tip of the windshield is constant and equal to the maximum force which would be required to buckle the plastic zone in the windshield under dynamic loading.

It is assumed that the force varies with obliquity in the same manner as the force which would be required to compress a short cylindrical plastic shell between frictionless surfaces. The force is thus assumed to be proportional to the function¹¹

$$\frac{\cos\theta}{\sqrt{1 + \frac{3}{4}\pi^2\sin^2\theta\cos^2\theta}}$$

Rotational equilibrium is maintained in the windshield by a bending moment M which is zero at the tip of the windshield and is greatest at the base. Since the length of a service type windshield is much greater than its swell radius, the bending moment at the base of the windshield becomes equal, at an early stage of an oblique impact, to the minimum value which is required to produce deformation or fracture of the windshield.

When the windshield is no longer rigidly attached to the projectile, the total force and torque on the windshield are no longer nearly zero, but are equal, instead, to the force and torque which are required to turn the windshield aside with some point near the base of the windshield for a pivot. The initial motion of the windshield, when under a force applied to its tip and a pivot reaction applied to its base, is the same as it would be if a solitary force were applied to the center of percussion in a direction which is perpendicular to the line joining the pivot, the center of mass, and the center of percussion. The line of action of this solitary force and the lines of action of any two component forces must have a common point of intersection. The resolution of forces on each part of the projectile is illustrated by Figures (1) to (4).

Just after the windshield has been demolished, a portion of the windshield still lies in the path of the projectile at low obliquity and may apply an appreciable amount of dynamic stress to the body as it is accelerated out of the path of the body.

A sample calculation of the windshield effect has been completed for the case of a 6" Comm Mk 27-7 projectile, and the results are given in Table I. The bending moment at the base of the windshield is less than the bending moment of plastic yielding until the unperforated part of the windshield reaches the plate. The windshield and the hood are then simultaneously pulled loose from the body and from each other if the obliquity is greater than 15° . The windshield finally turns about a pivot point near the outer edge of its base. The function θ_1 which has been selected to represent the windshield effect is tabulated in Table IV and the overall function which has been selected to represent the windshield effect, with both plastic and dynamic terms included, is summarized in Table V.

Performance on Normal Impact

During a slow compression a ductile windshield periodically buckles inward to form a succession of concentric folds. The force on the windshield fluctuates between two nearly constant limits. The force is a maximum when the windshield is just beginning to buckle, and is a minimum when each fold is half completed.

During a rapid compression the folds may not have time to develop. The material of the windshield continues to be compressed instead and flows outward until the flow stress in the material is equal to the fracture stress. The tip of the windshield is thus gradually fractured in a high velocity impact, and the force on the windshield may remain steadily at the upper limit which is required to buckle the windshield.

Performance on Oblique Impact

The behavior of the windshield in an oblique impact depends upon the design of the projectile. A 3" AP Mk '29-2 projectile or a 40mm AP M81A1 projectile buckles at the base of the windshield next to the threaded ring even at normal obliquity. A 5" Comm Mk 46-2 projectile may buckle at the base of the windshield if the windshield and threaded ring are all in one piece, but the threaded ring may first be pulled loose if the windshield and threaded ring are welded. A 6" Comm Mk '27-7 projectile apparently breaks first at the solder between the hood and the body, and the windshield and hood may then move together as a unit for a brief interval. The force moment at the base of the windshield quickly increases, however, until the threaded ring is pulled loose from the hood. The hood and windshield may then move as separate units, while the windshield probably buckles along one edge of the base where it presses against the hood.

Static Tests

The longitudinal force which is required to crush a windshield has been measured in the universal testing machine. In the case of a 3" AP Mk '29-2 projectile, the force on a steel windshield rose rapidly to an average value of 3000 pounds and then fluctuated periodically about the average with an amplitude of ± 1000 pounds. Each fluctuation could be correlated with the formation of a new concentric fold in the windshield. The average hardness of three steel windshields was 180 VPN, which corresponds to a tensile strength of $89000 \text{ (lb)/(in)}^2$. The force on an aluminum windshield rose to an average value of 8000 pounds and fluctuated with an amplitude of ± 4000 pounds. The aluminum windshield fractured gradually into many pieces instead of collapsing into concentric folds.

In the case of a 6" Comm Mk '27-7 projectile, the force rose rapidly at first to 20,000 pounds. The webs between the openings near the tip then collapsed and the force fell to 3000 pounds, where it stayed until the perforated zone near the tip was all folded under. The force then rose again to an average value of 33,000 pounds and fluctuated with an amplitude of $\pm 12,000$ pounds. The windshield is required by specifications to stand a compression load of 66,000 pounds at a section 5.1" in diameter. The compression stress would then be $44,000 \text{ (lb)/(in)}^2$. If this is the effective yield stress, then the windshield should not yield under a pure bending moment unless the bending moment is greater than $110,000 \text{ (lb)(in)}$. An individual 6" Comm Mk '27-7 projectile has been placed in a jig and has been subjected to a transverse load at the bourrelet. The hood broke loose from the body, and the threaded ring pulled loose simultaneously when the bending

moment at the base of the windshield was 105,000 (lb)(in). The bending moment for failure is known only for this stress distribution in a jig, and would probably be different if a compression load were applied simultaneously to the tip of the windshield. The average hardness of four windshields was 146 VPN which corresponds to a tensile strength of 74,000 (lb)/(in)². The tensile strength under dynamic loading is unknown, but is probably somewhere near the tensile strength for high tensile steel, which is estimated to be at least 100,000 (lb)/(in)².

Dynamic Tests

The windshields have not been recovered after impact at high striking energy. Evidence that the windshields may be fractured is to be found in a series of flash X-radiograms of windshields in flight, two of which are reproduced in Figures (5) and (6). A flash X-radiogram of stationary windshields after static compression is included in Figure (7) for comparison. That the maximum force on the windshield in a dynamic impact may be essentially the same as the maximum force in a static compression is proved by a comparison between flash X-radiograms in one of which the windshield had begun to buckle at the threaded ring. The windshield has been found to buckle at the same stage in a static compression.

The 40mm AP M81 projectile and the 40mm AP M81A1 projectile are, in reality, miniature common projectiles. The windshield of the 40mm AP M81 projectile is secured to the body by means of a hood, whereas the windshield of the 40mm AP M81A1 projectile is secured to the body by means of a crimping groove. A ballistic comparison between the projectiles has been made at the Plate Fuze Battery. The ballistic data are consistent with an appreciable dynamic term in the windshield effect at low obliquity. A quantitative comparison between these projectiles and monobloc projectiles is unfortunately obscured by an absence of records of the plate numbers which were tested. From existing records it may be inferred that the average tensile strength of the plates was 120,000 (lb)/(in)².

The ballistic data for miscellaneous common projectiles are listed in Table XI with the values of the windshield effect or the hood and windshield effects which are derived from Tables V and VI. The windshield effect for each projectile is assumed to be proportional to the percent mass of the windshield.

A ballistic investigation of the windshield effect has been made at the Armor and Projectile Laboratory with 3" AP Mk 29-2 projectiles against 0.25" plate at 0° obliquity. The ballistic data are summarized in Tables IX and X.

The limit energy required for penetration by a projectile with a windshield was much greater than the energy required by a projectile without a windshield. The difference in energy was 15000 ± 1000 (ft)(lb) for the actual ballistic test, whereas the energy required to collapse the windshield was found to be only 1200 (ft)(lb) for static loading. The recovered windshields had the same appearance for both ballistic and static compression, but the impact holes appeared to be changed by the presence of a windshield. The petals remained intact during near limit impacts, but the number of petals in each star crack was usually less for a projectile with a windshield than the number of petals for a projectile without a windshield. The energy required for penetration by a round nosed AP projectile without a windshield was also greater than the energy required by a pointed monobloc projectile, and the number of petals tended to be less for the round nosed projectile than for the pointed projectile. A collapsed windshield may possibly cushion the impact, or may so spread out the pressure on the plate that the type of fracture is changed. The large windshield effect tended to vanish as the striking energy was increased above the limit energy.

The absorption of energy during these tests increased slowly with increase in the striking energy when the striking energy was far above limit, but the armor in the path of the projectile takes up more and more kinetic energy which escapes with the petals if the petals break off, or enlarges the impact hole if the petals remain intact. Analogous results have been obtained at the Naval Research Laboratory with Cal. .50 and 37mm scale model projectiles in mild steel.

A ballistic investigation of the windshield effect has been made at the Plate Fuze Battery with 6" AP Mk 35-5 projectiles against 3" Class B plate at 40° obliquity. The ballistic data are summarized in Table XII.

THE HOOD EFFECT

The Dynamics of the Hood

The hood remains essentially undeformed if the plate is too thin to apply more pressure than the yield stress of the hood. The order of magnitude of the critical thickness of plate for destruction of the hood is given by the expression*

$$\left(\frac{1}{3}\right) \frac{X_1'}{X_0'} d$$

* The coefficient in this expression is valid for the 6" Comm Mk '27-7 projectile.

in which X'_1 is the effective yield stress of the hood and X'_0 is the effective yield stress of the plate.

The hood is too soft to penetrate a thick plate, but does apply enough pressure to the face of the plate to interfere with the elevation of a coronet.

The cross section of the hood increases from tip to base. The stress in the hood therefore decreases from tip to base and reaches the yield point at a short distance from the face of the plate. The plastic deformation of the hood is limited to a narrow zone next to the plate. Stress in the elastic zone is propagated with the velocity of sound which is much greater than the velocity of the projectile. The elastic zone is therefore essentially in equilibrium under the stresses which are applied to it by the plate and by the body.

There are two types of stress in the plastic zone, a plastic stress which deforms the material of the hood and a dynamic stress which accelerates the material of the hood out of the path of the projectile.

The hood is knocked loose from the body soon after the first instant of impact. The plastic stress in the crown at the edge of the plastic zone is therefore parallel to the surface of the crown, and is approximately coplanar with the vectors n and k .

In the limiting case of a low velocity impact, the distribution of stress in the crown is analogous to the distribution of stress around an expanding hole in a thin plate¹¹. The variable thickness h' of the crown has a maximum value¹⁰ of $(2.6)h$, and the plastic stress is approximately equal to the dynamic tensile strength in the region of maximum thickness.

The force and torque at the edge of the plastic zone are transmitted by the elastic zone to the body of the projectile. The plastic stress X'_1 in the crown therefore contributes a force on the body which is given by the expression

$$= (2.6)hX'_1 \oint \sqrt{\left(\frac{\partial x}{\partial \varphi}\right)^2 + \left(\frac{\partial y}{\partial \varphi}\right)^2} \frac{k - k \cdot nn}{\sqrt{1 - (k \cdot n)^2}} d\varphi$$

and contributes a torque on the body which is given by the expression

$$= (2.6)hX'_1 \oint \sqrt{\left(\frac{\partial x}{\partial \varphi}\right)^2 + \left(\frac{\partial y}{\partial \varphi}\right)^2} \frac{u}{\sqrt{1 - (k \cdot n)^2}} d\varphi$$

The function u in the expression for torque is defined by the equation

$$u = (b - \frac{\phi}{\cos\chi})\sin\chi + r \frac{\sin\phi}{\cos\chi} + \frac{k \cdot n}{R}(R - a)(b - \frac{\phi}{\cos\chi} + r\sin\phi\tan\chi)\sin\phi$$

and the torque is referred to an axis through the edge of the bourrelet. To the torque about this axis at the bourrelet must be added the torque between the bourrelet and the center of mass.

In the limiting case of a high velocity impact, the material of the crown flows away from the point of impact. That material of the crown which lies in a sector of width $d\phi$ flows locally like a flat jet of width $rd\phi$ and thickness h . The point of impact of the jet moves over the surface of the plate. The vector velocity v of the jet is reduced to the vector

$$\frac{k \cdot v}{k \cdot t} t$$

when the coordinates of the jet are referred to the moving point of impact. The rate of flow of mass in such a stationary jet is therefore given by the expression

$$- \frac{k \cdot v}{k \cdot t} \rho h r d\phi$$

in which ρ is the density of the material in the hood. The nose of the projectile applies a dynamic pressure which is collinear with n , and the plate applies a dynamic pressure which is collinear with $-k$. The change in the velocity of the stationary jet is collinear with the vector $n-k$, and the final velocity in the jet is orthogonal to k . The change in velocity is therefore equal to the vector

$$\frac{k \cdot v}{(1 - k \cdot n)}(n - k)$$

The dynamic stress in the hood contributes a force on the body which is given by the expression

$$+ \rho h (k \cdot v)^2 \oint \frac{r}{k \cdot t (1 - k \cdot n)} n d\phi$$

and contributes a torque on the body which is given by the expression

$$+ \rho h (k \cdot v)^2 (R-a) \oint \frac{1}{(1-k \cdot n)} r \frac{\partial r}{\partial \phi} \sin \phi d\phi$$

The torque is referred to an axis through the edge of the bourrelet. To this torque must be added the torque between the bourrelet and the center of mass. These integrals do not converge when n is collinear with k , and are not, therefore, valid at the tip of a round-nose projectile at any obliquity, or at the tip of a pointed projectile at high obliquity. The force and torque in such projectiles are limited by yielding of the plate.

The curvature of the nose contour gives the leading portion of the crown a greater radial velocity than the succeeding portions. The variation in radial velocity with distance from the nose of the projectile sets up a radial tension which tends to cancel the dynamic stress. The effect of dynamic stress on the motion of the projectile is probably not important unless there is more than enough kinetic energy in the crown to bring the material of the crown to the point of fracture.

When the skirt reaches the plate at low obliquity, it usually breaks into three or more pieces which are not further deformed. If cleavage of the skirt did not occur, the hood effect would be increased by a factor of the order of four. The pieces of the skirt apply a force on the body as long as they remain in contact with the body. The skirt probably therefore interferes with the penetration only in the case of a high velocity impact.

When the skirt reaches the plate at high obliquity it is trapped between the plate and the body and may be severely deformed if the plate is thick. The magnitude of the hood effect, which is associated with this plastic work, has been inferred from the ballistic data. Corrections for differences in the ogive effect were included in the analysis. The ogive effect was assumed to have its full value in the range $0^\circ \leq \theta \leq 45^\circ$, was assumed to be two thirds as large at $\theta = 50^\circ$, was assumed to be one third as large at $\theta = 55^\circ$, and was assumed to be zero in the range $60^\circ \leq \theta \leq 75^\circ$.

A sample calculation of the plastic hood effect has been completed for the 6" Comm Mk '27-7 projectile, and the results are given in Table II. The critical thickness of plate for extensive plastic deformation of the hood is estimated to be 1" at low obliquity, but the critical thickness is probably smaller at high obliquity as the result of dynamic stress in the armor. The dynamic stress in the hood is relatively unimportant unless the velocity of impact is greater than 750 (ft)/(sec). The limit which is approached by the dynamic hood effect at hypervelocity has been estimated for the case of the 6" Comm Mk '27-7 projectile, and the results are given in Table III. The crown and the skirt are both included in the estimate. The function Θ_2 which has been selected to represent the hood effect is tabulated in Table IV, and the overall function which has been selected to represent the hood effect, with both plastic and dynamic terms included, is summarized in Table VI.

Dynamic Tests

The plate penetration coefficients for jacketed small caliber projectiles increase with obliquity from 0° to 30° , whereas the plate penetration coefficients for monobloc projectiles decrease in this range of obliquity. The jacket effect seems to increase more rapidly with obliquity than the hood effect.

A 6" Comm Mk 27-7 projectile has been fired against STS plate No. 98503. The plate thickness was 1.91", the obliquity was 0° , and the striking velocity was 957 (ft)/(sec). The point of impact was surrounded by a concentric arrangement of a culvert pipe and an armor tube. The annular space between the culvert pipe and the armor tube was filled with sawdust. The fragments of the windshield and the hood were thus recovered without any evidence of secondary damage.

The windshield and the crown of the hood were splintered into many pieces, but the skirt of the hood was recovered in three equal pieces. The fractures in the hood belong to three distinct systems.

(1) The crown of the hood was fractured at the tip by circumferential tension. The fractures were propagated on that plane of maximum shear stress which contains the radial axis. Analogous fractures have been observed in cylindrical projectiles after impact¹¹.

(2) The crown of the hood was fractured at the free surface by radial tension. The fracture stress was set up by the radial flow of the crown away from the skirt. The fractures were propagated on that plane of maximum shear stress which contains the circumferential axis. Many of the fractures were propagated only part way through the crown, possibly as the result of a variation of ductility after flow under a variable hydrodynamic pressure. The incomplete fractures were opened up by flow after fracture, and the fragments of the crown have a stepped appearance. That the steps are not the result of a localization of shear strain between blocks of material is indicated by metallographic examination which shows no indication of local shear at the fracture surfaces.

(3) The skirt of the hood was fractured into three sectors by circumferential tension. The three fractures were initiated by three minute punched indentations on the shoulder of the hood, where the hood and windshield are locked together. Recognizable striae in the fracture surfaces radiate from the points of initiation. A fourth fracture was also observed which was not initiated by any obvious imperfection. The fractures were propagated in the skirt by brittle cleavage. Three of the cleavage fractures shifted to shear fractures when they ran into the severely worked

region of the crown. The propagation then followed that plane of maximum shear stress which contains the radial axis. That the fourth fracture failed to reach the crown is indicated by metallographic examination. Measurements of the fragments and coupon tests show that the reduction of area at the brittle fractures was not more than 2%, whereas the same material would undergo a reduction of area of more than 65% in a standard tensile test. The full reduction of area occurred after the fractures switched from cleavage to shear. Analogous brittle fractures have been observed in strips of mild steel^{1,2}.

The static tensile strength of the hood was 51000 (lb)/(in)². The dynamic tensile strength was probably 80000 (lb)/(in)². The crown was increased in thickness from .2" to more than .45" by plastic flow.

The hood of a 5" Comm Mk 46-2 projectile has been recovered intact after impact against STS plate No. 55276B. The plate thickness was .250", the obliquity was 70°, and the striking velocity was 654 (ft)/(sec).

The ballistic data for miscellaneous common projectiles are listed in Table XI, with the values of the windshield effect or the hood and windshield effects which are derived from Tables V and VI. The hood effect for each projectile is assumed to be proportional to the percent mass of the hood.

THE CAP EFFECT

The Dynamics of the Cap

The cap remains intact and attached to the body if the plate thickness is less than a lower critical thickness. The dynamics of the cap and body are then the same as the dynamics of a monobloc projectile with the same external contour.

The cap is knocked loose from the body but is deformed only near the skirt if the plate thickness is in an intermediate range of thickness. At low obliquity the cap is carried along by the body as though it were still attached to the body. At high obliquity the cap is pushed aside and the cap and body behave like a monobloc projectile with an offset nose. The effect is especially severe in the case of a 6" AP Mk 35-5 projectile which has an especially round nose, a long cap, and a large cap angle.

The cap shatters if the plate thickness is more than an upper critical thickness. The fragments of the cap are pushed aside by the body as it enters the plate. At low obliquity, the fragments deprive the body of a fraction of

its kinetic energy if the hardness of the cap exceeds the hardness of the plate. The effect is illustrated by the following table, which gives the percent increase in $F(e/d, \theta)$ per unit increase in the percent mass of the cap at 0° obliquity.

<u>Projectile</u>	<u>Cap hardness</u>	<u>Notch depth</u>	$(\frac{m}{m_s})(\frac{\Delta F}{F})$
8" AP Mk 11-1	230 VPN	small	.50
3" AP M62	540 VPN	large	.75
3" AP Type A	600 VPN	none	.60
37mm AP M51B2	800 VPN	large	.75

Absorption data which have been obtained by the Armor and Projectile Laboratory contain evidence that the fraction of the striking energy which is lost by the body because of the cap is nearly independent of striking energy.

The fragments of the shattered cap and the windshield seem to cushion the impact at low obliquity. The optimum hardness of the plate is greater for a capped projectile than the optimum hardness for an uncapped projectile.

At high obliquity, the fragments aid in the penetration of the plate if the hardness of the cap exceeds the hardness of the plate. The cap effect is influenced by the depth of the circumferential notch which holds the windshield. Caps which are unnotched or are lightly notched have less effect than caps which are deeply notched.

The sharp shoulder of the cap may scrape the plate severely at high obliquity. If the plate thickness is less than a critical thickness, the cap opens a longitudinal slit in the plate and the limit velocity for a capped AP projectile is consistent with the limit velocity of a pointed monobloc projectile, but if the plate thickness is more than the critical thickness, the cap opens transverse cracks and the limit velocity is low. The appearance of the impacts is illustrated by Figures (10) and (11). At the critical plate thickness, the projectile has a component of velocity parallel to the plate which is nearly equal to the velocity of propagation of a plastic undulation. The cap can bite the plate only if the projectile can overtake the undulation.

The functions which have been selected to represent the cap effect are summarized in Tables VII and VIII.

Ballistic Tests

Decapping action by the plate has been recorded in a few flash X-radio-graphs, and by a systematic study of recovered fragments at the Armor and Projectile Laboratory. The data are summarized in Table XV. Decapping action has been detected at the Plate Battery with yaw cards and movie cameras set up behind the plate. Caps have occasionally been recovered in the butts at the Plate Battery or stuck in the plate. The data are summarized in Table XVI. The occurrence of shatter in the cap can be detected by the presence of characteristic dents and scrapes in the impact hole. The appearance of the impact holes is illustrated by Figures (8) and (9).

Comparative limit determinations which have been made at the Princeton Station with 20mm capped and uncapped projectiles are consistent with data which have been obtained at the Armor and Projectile Laboratory with 3" AP projectiles and at the Plate Battery with 8" AP projectiles. The ballistic data are summarized in Tables XIII and XIV. The cushioning effect of the cap and windshield is illustrated by the data for the 8" AP Mk 19-5 projectile against 5.2" Class B plate No. 9473. The limit velocity at 0° obliquity for the capped 8" AP Mk 19-5 projectile was consistent with other limit velocities for capped 8" AP Mk 19-6 projectiles in a range of plate thickness from 3.6" to 10.6", yet the limit velocity for an uncapped 8" AP Mk 19-5 projectile was 12% low with respect to the limit velocity for a ductile plate.

APPENDIX A

APPENDIX A

Indefinite integrals which enter into the analysis of an ogival surface.

Surface

$$s = 2\pi R \int \frac{rdr}{\sqrt{R^2 - (R-a+r)^2}} = -2\pi R \left\{ (b-z) + (R-a) \cos^{-1} \frac{1}{R}(b-z) \right\}$$

Center of mass

$$\int (b-z) ds = -2\pi R \int r dr = \pi R r^2$$

Radius of gyration

$$\int \left\{ (b-z)^2 + \frac{1}{2} r^2 \right\} ds = -\frac{2}{3} \pi R (b-z)^3$$

$$- \frac{1}{6} \pi R \{ 2r^2 + (R-a)r + 21R^2 - 34aR + 17a^2 \} (b-z)$$

$$- \frac{1}{2} \pi R (R-a) (7R^2 - 4aR + 2a^2) \cos^{-1} \frac{1}{R}(b-z)$$

APPENDIX B

APPENDIX B

Indefinite integrals which enter into the analysis of an ogival volume.

Volume

$$\tau = \pi \int r^2 dz = \frac{1}{3} \pi (b-z)^3 + \pi \{ (R-a)r - R^2 \} (b-z) - \pi R^2 (R-a) \cos^{-1} \frac{1}{R} (b-z)$$

Center of mass

$$\pi \int (b-z) r^2 dz = \pi \left\{ \frac{1}{3} (R-a) r^3 + \frac{1}{4} r^4 \right\}$$

Radius of gyration

$$\begin{aligned} \pi \int \left\{ (b-z)^2 + \frac{1}{4} r^2 \right\} r^2 dz &= + \frac{3}{20} \pi (b-z)^5 \\ &+ \frac{1}{12} \pi \{ 3(R-a)r + 3R^2 - 10aR + 5a^2 \} (b-z)^3 \\ &+ \frac{1}{8} \pi \{ (R-a)(7R^2 - 8aR + 4a^2)r - 9R^4 + 10R^3a + 3R^2a^2 - 8Ra^3 + 2a^4 \} (b-z) \\ &- \frac{1}{8} \pi R^2 (R-a)(9R^2 - 8aR + 4a^2) \cos^{-1} \frac{1}{R} (b-z) \end{aligned}$$

APPENDIX C

TABLE I

Theoretical values for the windshield effects of the 6" Comm Mk '27-7 projectile, calculated with the mass and radius of gyration of the body.

θ	$(10^{-8})v_s^2 \left(\frac{\Delta w}{\frac{1}{2}mv_s^2} \right)$	$(10^{-8})v_s^2 \Delta \theta$	$(10^{-8})v_s^2 \Delta \chi$	$(10^{-8})v_s^2 \left(\frac{d\Delta \dot{\chi}}{v_s} \right)$
	(ft) ² /(sec) ²	(ft) ² /(sec) ²	(ft) ² /(sec) ²	(ft) ² /(sec) ²
0	(-.027)	(.000)	(.000)	(.000)
15	(-.021) -.019	(+.003) +.004	(+.006) +.015	(+.009) +.022
30	-.014	+.0035	+.011	+.016
45	-.009	+.003	+.008	+.012
60	-.006	+.002	+.006	+.009
75	-.003	+.001	+.003	+.005
90	.000	.000	.000	.000

Numbers in parentheses refer to a projectile with the windshield rigidly attached to the body.

TABLE II

Theoretical values for the hood effects of the 6" Comm Mk 27-7 projectile at striking velocities less than 750 (ft)/(sec)

θ	$(10^{-6})v_s^2\left(\frac{\Delta w}{\frac{1}{2}mv_s^2}\right)$	$(10^{-6})v_s^2\Delta\theta$	$(10^{-6})v_s^2\Delta\chi$	$(10^{-6})v_s^2\left(\frac{d\Delta\chi}{v_s}\right)$
	(ft) ² /(sec) ²	(ft) ² /(sec) ²	(ft) ² /(sec) ²	(ft) ² /(sec) ²
0	-.047	.000	.000	.000
15	-.032	+.002	+.001	+.005
30	-.019	+.003	+.001	+.007
45	-.007	+.002	+.000	+.005

TABLE III

Theoretical values for the hood effects of the 6" Comm Mk 27-7 projectile at hypervelocity.

θ	$\frac{\Delta w}{\frac{1}{2}mv_s^2}$	$\frac{1}{\sin\theta}\Delta\theta$	$\frac{1}{\sin\theta}\Delta\chi$	$\frac{d}{\sin\theta}\frac{\Delta\chi}{v_s}$
$\leq 45^\circ$	-.05	+.07	+.01	+.125

TABLE IV

The function θ_1 in the windshield effect and the function θ_2 in the hood effect of the 6" Comm Mk 27-7 projectile at impact velocities less than 750 (ft)/(sec).

θ	$(10^{-8})\theta_1$	$(10^{-8})\theta_2$
0	.114	.200
15	.137	.147
20	.137	.130
25	.135	.114
30	.130	.097
35	.124	.081
40	.116	.067
45	.105	.084
50	.089	.134
55	.065	.150
60	.041	.112
65	.021	.055
70	.010	.015
75	.005	.006

TABLE V

The windshield effect of the 6" Comm Mk 27-7 projectile in Class B armor or STS. The windshield is 5.1% of the total mass of the projectile.

$$\frac{\Delta F}{F}$$

$\frac{e}{d}$	θ							
	0	15	20	25	30	35	40	45
.1	.228	.278	.285	.292	.295	.299	.292	.264
.15	.120	.143	.146	.149	.151	.152	.149	.136
.2	.078	.091	.093	.095	.096	.097	.096	.088
.3	.050	.056	.057	.058	.059	.059	.058	.055
.4	.042	.045	.045	.045	.046	.047	.049	.049
.5	.042	.043	.043	.044	.045	.047	.052	.055
.6	.045	.045	.045	.046	.048	.052	.059	.068
.7	.050	.050	.050	.051	.053	.058	.067	.082
.8	.055	.055	.055	.056	.059	.064	.074	.093
.9	.059	.059	.059	.060	.063	.069	.080	.100
1.0	.061	.061	.061	.062	.066	.072	.083	.105

TABLE V (Continued)

$\frac{e}{d}$	$\frac{\Delta F}{F}$					
	θ					
	50	55	60	65	70	75
.03			.236	.112	.070	.053
.05		.302	.150	.078	.052	.042
.075	.311	.185	.102	.059	.043	.036
.10	.201	.129	.078	.049	.038	.033
.15	.110	.078	.054	.038	.032	.030
.20	.074	.056	.043	.033	.030	.028
.30	.048	.040	.033	.029	.027	.027
.40	.042	.035	.030	.028	.027	.026
.50	.043	.033	.029	.027	.026	.026

TABLE VI

The hood effect of the 6" Comm Mk 27-7 projectile in Class B armor or STS.
The hood is 5.2% of the total mass of the projectile.

$$\frac{\Delta F}{F}$$

$\frac{e}{d}$	θ							
	0	15	20	25	30	35	40	45
.1	.382	.297	.272	.251	.227	.205	.180	.217
.15	.191	.152	.140	.130	.120	.109	.098	.114
.2	.119	.097	.090	.085	.079	.073	.066	.076
.3	.069	.059	.056	.053	.050	.047	.045	.049
.4	.054	.048	.046	.044	.043	.044	.047	.051
.5	.052	.047	.046	.046	.047	.050	.057	.065
.6	.055	.052	.051	.051	.054	.059	.068	.082
.7	.061	.058	.058	.059	.063	.070	.081	.098
.8	.067	.065	.065	.066	.070	.077	.088	.110
.9	.071	.070	.070	.072	.075	.082	.095	.118
1.0	.073	.073	.073	.074	.078	.085	.098	.123

TABLE VI (Continued)

$\frac{e}{d}$	$\frac{\Delta F}{F}$					
	θ					
	50	55	60	65	70	75
.03			(.614)	(.270)	(.089)	(.059)
.05		(.663)	(.376)	(.172)	(.064)	(.046)
.075	(.455)	(.394)	(.240)	(.120)	(.050)	(.039)
.10	.291	.264	.171	.090	.043	.035
.15	.153	.147	.103	.061	.035	.031
.20	.098	.097	.073	.047	.032	.029
.30	.060	.059	.047	.036	.029	.027
.40	.051	.046	.038	.030	.027	.027
.50	.059	.047	.037	.029	.026	.026

The numbers in parentheses refer to plate thicknesses for which the hood is usually undeformed.

TABLE VII

The cap effect of the 3" AP M62 projectile in Class B armor or STS. The cap is 13.9% of the total mass of the projectile, the cap is deeply notched to hold a windshield, and the hardness is 50R_c. Projectiles are decapped at $e/d \geq .16$. Decapped projectiles with caps intact show no indication of a cap effect.

Projectiles with shattered caps

	θ										
	0	15	20	25	30	35	40	45	50	55	≥ 60
min											
$\frac{e}{d}$.53	.48	.46	.45	.43	.41	.40	.38	.37	.35	$\leq .34$
$\frac{\Delta F}{F}$.104	.115	.125	.137	.151	.165	.173	.153	.097	.035	.000

TABLE VIII

The cap effect of the 6" AP Mk 35-5 projectile in Class B armor or STS. The cap is 20% of the total mass of the projectile, the cap is slightly notched to hold a windshield, and the average hardness is 53R_C. Projectiles are decapped at $e/d \geq .08$.

Decapped projectiles with caps intact

	θ							
	≤ 40	40	50	55	60	65	70	≥ 75
max $\frac{e}{d}$	$\geq .50$.48	.46	.44	.43	.42	.42	.42
$\frac{\Delta F}{F}$.000	.015	.055	.082	.070	.032	.005	.000

Projectiles with shattered caps

	θ								
	0	15	20	25	30	35	40	45	50
min $\frac{e}{d}$.66	.60	.58	.56	.54	.52	.50	.48	$\leq .46$
$\frac{\Delta F}{F}$.120	.131	.141	.153	.167	.177	.146	.055	.000

APPENDIX D

CONFIDENTIAL

NPC REPORT NO. 1211

BALLISTIC DATATABLE IX

Absorption Data for Various Projectiles in Thin Mild Steel Plate at 0° Obliquity

Projectile	Plate Number	Plate Tensile Strength	$\frac{e}{d}$	$(10^{-8})F_S^2$	$(10^{-8})F_R^2$	$F\left(\frac{e}{d}, \theta\right)$	Average Plate Condition
3" AP M79	-	65000 ± 3000	.093	3.2 ± .1	0	17800 ± 400	4- petal star, petals intact
"			.089	155	150 ± 1		7- petal star, petals broken
"			.089	429	415 ± 1		8- petal star, petals intact
3" AP Mk 29-2 + Ws	-	"	.093	11.3 ± .3	0	33600 ± 400	3- petal star, petals intact
"			.088	143	129 ± 1		5- petal star, petals broken
"			.088	389	365 ± 1		petals wiped
3" AP Mk 29-2 - Ws	-	"	.092	4.4 ± .3	0	21000 ± 700	4- petal star, petals intact
"			.088	135	123		punching thrown
"			.089	367	339 ± 1		punching thrown
3" Comm Mk 3 - 7	-	"	.082	3.5 ± .2	0	18700 ± 500	4- petal star, petals intact

CONFIDENTIAL

CONFIDENTIAL

BALLISTIC DATA

TABLE X

Absorption Data for Various Projectiles in Thin STS at 0° Obliquity

Projectile	Plate Number	Plate Tensile Strength	$\frac{e}{d}$	$(10^{-8})F_3^2$	$(10^{-8})F_P^2$	$F(\frac{e}{d}, \theta)$	Average Plate Condition
3" AP M79	7404A	121000	.084	144	138 ± 1		5- petal star, petals broken petals wiped
"	"	"	.084	465	451 ± 2		
3" AP Mk 29-1+Ws	"	"	.084	417	390 ± 2		8- petal star, petals intact punching thrown
"	"	"	.084	404	374 ± 1		
3" AP Mk 29-1-Ws	"	"	.083	153	135 ± 1		6- petal star, petals intact
3" AP Mk 29-2+Ws	"	"	.084	418	386		6- petal star, petals broken punching thrown
"	"	"	.084	136	124 ± 1		punching thrown
3" AP Mk 29-2-Ws	"	"	.083	407	379		punching thrown
"	"	"	.083	4.6 ± .2	0	21500 ± 500	4- petal star, punching started*
3" Comm Mk 3-7	"	"	.084	408	373		punching thrown
3" AP Expr. (flat nose +Ws)	"	"	.085	3.7 ± .2	0	19300 ± 500	4- petal star, petals intact
3" AP M79	158494	107000	.085	14.2 ± .8	0	37700 ± 1000	2- petal star, petals intact
3" AP Mk 29-2+Ws	"	"	.085	7.3 ± .2	0	27000 ± 300	3- petal star, petals intact
3" AP Mk 29-2-Ws	"	"	.064	256	232 ± 2		5- petal star, petals broken
4" Comm Mk 16-1	"	"	.064	388	371 ± 2		5- petal star, petals intact

* Miniature punching with the same diameter as the flattened tip of the 3" Comm projectile.

CONFIDENTIAL

CONFIDENTIAL

TABLE XI

Plate Penetration Coefficients for Common Projectiles in Class B Armor or STS

Projectile	%Hd	%Ws*	Plate Number	Plate Tensile Strength	θ	$\frac{e}{d}$	$F(\frac{e}{d}, \theta)$	$\frac{\Delta F}{F}$ Calc.
5" Comm Expr. Type A+Ws	-	-	262833	-	30°	.200	≥30500	-
5" Comm Expr. Type A-Ws	-	-	"	-	30°	.200	30000 ± 500	-
5" Comm Expr. Type A+Ws	-	-	"	-	60°	.188	40700 ± 700	-
5" Comm Expr. Type A-Ws	-	-	"	-	60°	.188	≤37900	-
5" Comm Mk 29-1 + Ws	-	-	73774	-	30°	.283	38000 ± 1000	-
5" Comm Mk 29-1 - Ws	-	-	"	-	30°	.283	≤38000	-
5" Comm Expr. LW 5547-Hd+Ws	5.0	3.4	HH562	114000	24.5°	.606	46300 ± 200	.082
5" Comm Expr. DW 5547-Hd-Ws	"	"	"	"	25°	.600	42800 ± 100	-
5" Comm Expr. DW 5550-Hd+Ws	7.2	7.0	"	"	25°	.600	47200 ± 200	.136
5" Comm Expr. DW 5550-Hd-Ws	"	"	"	"	25°	.600	43500 ± 200	-
6" Comm Mk 27-4 - Hd-Ws	6.5	5.1	DD319	108000	0°	.910	47000 ± 1000	-
6" Comm Mk 27-1 + Hd+Ws	4.0	5.1	338053	116000	15°	.510	44000 ± 100	.047
6" Comm Mk 27-1 + Hd-Ws	"	"	"	"	15°	.510	42400 ± 100	-
6" Comm Mk 27-1 + Hd-Ws	"	"	37813**	122000	16°	.480	37800 ± 100	.035
6" Comm Mk 27-1 - Hd-Ws	"	"	"	"	14°	.480	37000 ± 300	-
6" Comm Mk 27-3 + Hd+Ws	6.5	5.1	GG292	116000	30.5°	.448	42000 ± 500	.098
6" Comm Mk 27-3 - Hd-Ws	"	"	"	"	29.5°	.448	38000 ± 1000	-

*With threaded ring included

**Laminated Plate

CONFIDENTIAL

CONFIDENTIAL

TABLE XI (Continued)

Projectile	ϕ_{Hd}	ϕ_{Ws}^*	Plate Number	Plate Tensile Strength	θ	$\frac{e}{d}$	$F(\frac{e}{d}, \theta)$	$\frac{\Delta F}{F}$	Calc.
6" Comm Mk 27-3 + Hd+Ws	6.5	5.1	G3296	117000	30°	.411	40500 ± 800	.100	
6" Comm Mk 27-3 - Hd-Ws	"	"	"	"	30°	.417	35500 ± 500		
6" Comm Mk 27-3 + Hd+Ws	"	"	G3928	124000	30°	.494	39500 ± 500	-	
6" Comm Mk 27-7 + Hd+Ws	5.2	5.1	F1823	128000	45°	.242	35600 ± 600	.128	
6" Comm Mk 27-7 - Hd-Ws	"	"	"	"	45°	.242	30100 ± 900		
6" Comm Mk 27-7 + Hd+Ws	"	"	NN25	119000	45°	.522	43300 ± 900	.125	
6" Comm Mk 27-7 - Hd-Ws	"	"	"	"	45°	.522	39600 ± 1100		
6" Comm Mk 27-7 + Hd+Ws	"	"	634580	124000	51°	.162	32200 ± 700	.224	
6" Comm Mk 27-7 - Hd-Ws	"	"	"	"	51°	.162	26600 ± 400		
6" Comm Mk 27-7 + Hd+Ws	"	"	09465	126000	50°	.162	37300 ± 600	.234	
6" Comm Mk 27-7 - Hd-Ws	"	"	"	"	50°	.162	32700 ± 2500		
6" Comm Mk 27-7 + Hd+Ws	"	"	75446	121000	50°	.408	41700 ± 900	.093	
6" Comm Mk 27-7 - Hd-Ws	"	"	"	"	49°	.408	38300 ± 400		
6" Comm Mk 27-7 + Hd+Ws	"	"	23164	124000	60°	.127	35800 ± 500	.190	
6" Comm Mk 27-7 - Hd-Ws	"	"	"	"	60°	.127	30500 ± 900		
6" Comm Mk 27-7 + Hd+Ws	"	"	X20580	123000	60°	.329	45500 ± 400	.067	
6" Comm Mk 27-7 - Hd-Ws	"	"	"	"	60°	.329	45700 ± 1000		

CONFIDENTIAL

CONFIDENTIAL

NPG REPORT NO. 1211

TABLE XI (Continued)

Projectile	%Hd	%Ws*	Plate Number	Plate Tensile Strength	θ	$\frac{e}{d}$	$F(\frac{e}{d}, \theta)$	$\frac{\Delta F}{F}$ Calc.
6" Comm Mk 27-7 + Hd+Ws	5.2	5.1	28909B	128000	75°	.0417	≥24800	.093
6" Comm Mk 27-7 - Hd-Ws	"	"	"	"	75°	.0417	22900 ± 900	
6" Comm Mk 27-7 + Hd+Ws	"	"	02027	129000	75°	.199	≥30700	.057
6" Comm Mk 27-7 - Hd-Ws	"	"	"	"	75°	.199	≥29400	
6" Comm Mk 27-7 + Hd+Ws	"	"	20137	123000	75°	.200	≥30500	.057
6" Comm Mk 27-7 - Hd-Ws	"	"	"	"	75°	.200	30800 ± 700	
8" Comm Mk 17-3 + Hd+Ws	3.7	3.5	1E253A1	103000	15°	.586	44500 ± 500	.031
8" Comm Mk 17-3 + Hd-Ws	"	"	"	"	15°	.586	43500 ± 500	

CONFIDENTIAL

CONFIDENTIAL

NPG REPORT NO. 1211

TABLE XII

Plate Penetration Coefficients for 6" AP Projectiles in Class B Armor

Projectile	$\frac{W}{s}$	Plate Number	Plate Tensile Strength	θ	$\frac{e}{d}$	$F(\frac{e}{d}, \theta)$	$\frac{\Delta F}{F}$	Calc.
6" AP Mk 35-5 + Ws	2.3	051662	118000	40°	.498	46100 ± 800		.024
6" AP Mk 35-5 - Ws	"	"	"	40.5°	.500	≥45200		
6" AP Mk 35-5 + Ws	"	051663	121000	41°	.500	45300 ± 400		.024
6" AP Mk 35-5 - Ws	"	"	"	40°	.500	41100 ± 900		
6" AP Mk 35-5 + Ws	"	12315	114000	40°	.527	45100 ± 1000		.025
6" AP Mk 35-5 - Ws	"	"	"	40°	.522	43400 ± 800		
6" AP Mk 35-5 + Ws	"	54B424B3	114000	40°	.486	44900 ± 2200		.024
6" AP Mk 35-5 - Ws	"	"	"	40°	.492	41200 ± 500		
6" AP Mk 35-5 + Ws	"	55K505B3	119000	40.5°	.524	44900 ± 1000		.025
6" AP Mk 35-5 - Ws	"	"	"	41°	.532	≥42800		

CONFIDENTIAL

CONFIDENTIAL

NPG REPORT NO. 1211

TABLE XIII

Plate Penetration Coefficients for 8" AP Projectiles in Class B Armor or STS

Projectile	Plate Number	Plate Tensile Strength	θ	$\frac{e}{d}$	$F(\frac{e}{d}, \theta)$
8" AP Mk 11-1 + cap	DD319	108000	0°	.683	45500 ± 1000
8" AP Mk 11-1 + cap	DD319	108000	36°	.370	36200 ± 200
8" AP Mk 11-1 + cap	DD319	108000	37°	.334	36000 ± 200
8" AP Mk 19-1 + Ws	DD319	108000	8°	.815	53700 ± 500
8" AP Mk 19-1 - Ws	DD319	108000	5°	.683	51000 ± 2000
8" AP Mk 11-1 + cap	9473	107000	3°	.656	45900 ± 300
8" AP Mk 11-1 + cap	9473	107000	29.5°	.653	43700 ± 500
8" AP Mk 19-1 + cap	9473	107000	0°	.650	53400 ± 1000
8" AP Mk 19-1 - cap	9473	107000	0°	.650	42000 ± 300
8" AP Mk 19-1 + cap	9473	107000	30°	.650	49100 ± 300
8" AP Mk 19-1 - cap	9473	107000	30°	.650	40100 ± 500
8" AP Mk 19-5 + cap	9473	107000	0°	.650	50600 ± 300
8" AP Mk 19-5 - cap	9473	107000	0°	.650	40500 ± 300
8" AP Mk 19-5 + cap	9473	107000	30°	.650	49800 ± 500
8" AP Mk 19-5 - cap	9473	107000	30°	.650	40800 ± 300
8" AP Mk 19-5 + cap	9563	111000	30°	.650	51200 ± 500
8" AP Mk 19-5 - cap	9563	111000	30°	.650	42200 ± 300

CONFIDENTIAL

TABLE XIII

Plate Penetration Coefficients for 8" AP Projectiles in Class B Armor or STS

Projectile	Plate Number	Plate Tensile Strength	θ	$\frac{e}{d}$	$F(\frac{e}{d}, \theta)$
8" AP Mk 11-1 + cap	DD319	108000	0°	.683	45500 ± 1000
8" AP Mk 11-1 + cap	DD319	108000	36°	.370	36200 ± 200
8" AP Mk 11-1 + cap	DD319	108000	37°	.334	36000 ± 200
8" AP Mk 19-1 + Ws	DD319	108000	8°	.815	53700 ± 500
8" AP Mk 19-1 - Ws	DD319	108000	5°	.683	51000 ± 2000
8" AP Mk 11-1 + cap	9473	107000	3°	.656	45900 ± 300
8" AP Mk 11-1 + cap	9473	107000	29.5°	.653	43700 ± 500
8" AP Mk 19-1 + cap	9473	107000	0°	.650	53400 ± 1000
8" AP Mk 19-1 - cap	9473	107000	0°	.650	48000 ± 300
8" AP Mk 19-1 + cap	9473	107000	30°	.650	49100 ± 300
8" AP Mk 19-1 - cap	9473	107000	30°	.650	40100 ± 500
8" AP Mk 19-5 + cap	9473	107000	0°	.650	50600 ± 300
8" AP Mk 19-5 - cap	9473	107000	0°	.650	40500 ± 300
8" AP Mk 19-5 + cap	9473	107000	30°	.650	49800 ± 500
8" AP Mk 19-5 - cap	9473	107000	30°	.650	40800 ± 300
8" AP Mk 19-5 + cap	9563	111000	30°	.650	51200 ± 500
8" AP Mk 19-5 - cap	9563	111000	30°	.650	42200 ± 300

CONFIDENTIAL

NPG REPORT NO. 1211

TABLE XIII (Continued)

Projectile	Plate Number	Plate Tensile Strength	θ	$\frac{c}{d}$	$F(\frac{c}{d}, \theta)$
8" AP Mk 19-5 + cap	9563	111000	40°	.650	49100 ± 300
8" AP Mk 19-1 + cap	128750	119000	50.2°	.37	≥43600
8" AP Mk 19-1 - cap	128750	119000	50.5°	.37	≤41300
8" AP Mk 11-1 + cap	21045	126000	30°	.240	35500 ± 200
8" AP Mk 11-1 - cap	21045	126000	30°	.240	30300 ± 300
8" AP Mk 11-1 + cap	X3323	128000	30°	.255	34000 ± 1000
8" AP Mk 11-1 - cap	X3323	128000	30°	.255	29200 ± 300
8" AP Mk 11-1 + cap	X4842	122000	31°	.345	36400 ± 200
8" AP Mk 11-1 - cap	X4842	122000	31.5°	.345	34000 ± 500
8" AP Mk 11-1 + cap	X5700	123000	30°	.348	35200 ± 200
8" AP Mk 11-1 - cap	X5700	123000	30°	.348	34600 ± 300
8" AP Mk 11-1 + cap	X6615	122000	30°	.316	38000 ± 500
8" AP Mk 11-1 - cap	X6615	122000	30°	.316	32000 ± 500
8" AP Mk 11-1 + cap	X6683	115000	30°	.406	38000 ± 300
8" AP Mk 11-1 - cap	X6683	115000	30°	.403	37200 ± 300
8" AP Mk 11-1 + cap	HHL35	119000	1.5°	.380	43000 ± 500
8" AP Mk 11-1 - cap	HHL35	119000	0°	.381	41000 ± 500
8" AP Mk 11-1 + cap	HHL35	119000	30°	.38C	37400 ± 200
8" AP Mk 11-1 - cap	HHL35	119000	30°	.380	≤35000

CONFIDENTIAL

CONFIDENTIAL

NPG REPORT NO. 1211

TABLE XIII Continued

Projectile	Plate Number	Plate Tensile Strength	θ	$\frac{e}{d}$	$F(\frac{e}{d}, \theta)$
8" AP Mk 11-1 + cap	HH161	116000	0°	.376	43000 ± 1500
8" AP Mk 11-1 + cap	HH161	116000	30°	.376	40000 ± 500
8" AP Mk 11-1 + cap	HH161	130000	0°	.364	43000 ± 500
8" AP Mk 11-1 + cap	HH161	130000	30°	.364	36000 ± 500
8" AP Mk 11-1 + cap	G3928	123000	31°	.371	32700 ± 200

CONFIDENTIAL

TABLE XIV

Plate Penetration Coefficients for 37mm and 3" AP Projectiles in Class B Armor or STS

Projectile	Plate Number	Plate Tensile Strength	θ	$\frac{e}{d}$	Uncorrected $F(\frac{e}{d}, \theta)$
3" AP Type A + cap	1478	123000	2.5°	.651	51500 ± 500
3" AP Type A - cap	1478	123000	5.5°	.652	46500 ± 500
3" AP Type A + cap	1478	123000	29°	.652	47300 ± 500
3" AP Type A - cap	1478	123000	29.5°	.652	44000 ± 1000
3" AP Type A + cap	1478	122000	45°	.652	47000 ± 1000
3" AP Mk 29-1	1478	123000	41°	.655	54000 ± 200
3" AP Type A-1	6858	107000	26°	1.739	54500 ± 200
3" AP Type A-1	6859	110000	30.3°	1.165	50500 ± 500
37mm AP M51B2 + cap	8333*	98500	1°	.754	54700 ± 300
37mm AP M51B2 + cap	8333**	98500	1°	.754	54200 ± 400
37mm AP M51B2 - cap	8333**	98500	1°	.754	47400 ± 500
3" AP M62 BS	10359	91000	30°	1.223	52100 ± 1000
3" AP M62 BS	10359	91000	35°	1.237	52500 ± 200
37mm AP M51B2 + cap	10650	104000	0°	1.380	57800 ± 200
3" AP M62 CHEV	10650	104000	30°	.669	51500 ± 600

* Section from surface of a 10.6" plate

** center " " " "

CONFIDENTIAL

NPG REPORT NO. 1211

TABLE XIV (Continued)

Projectile	Plate Number	Plate Tensile Strength	θ	$\frac{e}{d}$	Uncorrected $F(\frac{e}{d}, \theta)$
37mm AP M51B2 + cap	10650	128000	0°	1.380	5900 ± 400
3" AP M62 CHEV	10650	128000	30°	.671	53100 ± 500
3" AP M62 CHEV	12764	124000	20°	1.337	64400 ± 900
3" AP Mk 29-2	12764	124000	20°	1.396	59000 ± 700
3" AP Mk 29-2	23115	115000	0°	.165	34500 ± 300
3" AP Mk 29-2	23115	115000	30°	.165	29500 ± 300
3" AP Mk 29-2	23115	115000	45°	.165	30500 ± 300
3" AP Mk 29-2	23115	115000	59.8°	.164	30200 ± 300
3" AP Expr Mk 29 (flat nose + Ws)	23115	115000	.5°	.165	34300 ± 200
3" AP Expr Mk 29 (flat nose + Ws)	23115	115000	30°	.166	23100 ± 200
3" AP Expr Mk 29 (flat nose + Ws)	23115	115000	45°	.165	21000 ± 300
3" AP Expr Mk 29 (flat nose + Ws)	23115	115000	60.2°	.164	19900 ± 300
3" AP Type A	25074	124000	18.5°	.498	49000 ± 500
3" AP Type A	25752	128000	0°	.496	49500 ± 500
37mm AP M51B2 + cap	40228	105000	.5°	1.38	56400 ± 300
37mm AP M51B2 - cap	40228	105000	1°	1.379	50400 ± 300

CONFIDENTIAL

CONFIDENTIAL

NPG REPORT NO. 1211

TABLE XIV (Continued)

Projectile	Plate Number	Plate Tensile Strength	θ	$\frac{e}{d}$	Uncorrected $F(\frac{e}{d}, \theta)$
3" AP M62 CHEV	40228	103000	30°	.673	50300 ± 200
37mm AP M51B2 + cap	40228	128000	1°	1.394	57800 ± 200
37mm AP M51B2 - cap	40228	128000	1°	1.392	53400 ± 300
3" AP M62 CHEV	40228	119000	30°	.672	50400 ± 200
37mm AP M51B2 + cap	40497	86000	1°	1.014	53600 ± 200
37mm AP M51B2 - cap	40497	86000	.5°	1.018	45900 ± 200
37mm AP M51B2 + cap	40497	112000	.5°	1.007	55400 ± 100
37mm AP M51B2 - cap	40497	112000	.5°	1.007	50100 ± 100
37mm AP M51B2 + cap	40498	123000	1°	1.036	57300 ± 200
37mm AP M51B2 - cap	40498	123000	1°	1.036	51300 ± 100
37mm AP M51B2 + cap	40499	130000	1°	1.029	57300 ± 200
37mm AP M51B2 - cap	40499	130000	.5°	1.036	51900 ± 200
37mm AP M51B2 + cap	40500	120000	1°	1.009	55700 ± 100
37mm AP M51B2 - cap	40500	120000	2°	1.005	50900 ± 100
37mm AP M51B2 + cap	40502	105000	1.5°	1.012	54000 ± 100
37mm AP M51B2 - cap	40502	105000	1°	1.017	48800 ± 500

CONFIDENTIAL

CONFIDENTIAL

NPG REPORT NO. 1211

TABLE XIV (Continued)

Projectile	Plate Number	Plate Tensile Strength	θ	$\frac{e}{d}$	Uncorrected $F(\frac{e}{d}, \theta)$
3" AP M62 BS	40497	114000	40°	.496	249600
3" AP M62 BS	40497	114000	50°	.496	48400 ± 800
3" AP M62 BS	40497	114000	60°	.496	50600 ± 600
3" AP M62 BS	40498	110000	0°	.511	44600 ± 400
3" AP M62 BS	40498	110000	20°	.494	52100 ± 200
3" AP M62 BS	40498	110000	30°	.494	48200 ± 200
3" AP M62 BS	40498	109000	40°	.500	48400 ± 400
3" AP M62 BS	40500	120000	30°	.489	49100 ± 200
3" AP M62 BS	40502	105000	0°	.490	42700 ± 100
3" AP M62 BS	40502	105000	30°	.486	47700 ± 300
3" AP M62 BS	40502	105000	45°	.489	46900 ± 200
3" AP Mk 29-1	40917	124000	45°	.497	44800 ± 1000
3" AP Mk 29-2	40917	124000	1°	.493	51700 ± 200
3" AP Mk 29-2	40917	124000	30°	.495	49600 ± 200
3" AP Mk 29-2	40917	124000	45°	.499	47700 ± 800
3" AP Mk 29-2	40917	124000	60°	.498	52900 ± 1000
3" AP Expr Mk 29 (flat nose + Ws)	40917	124000	1°	.498	38800 ± 400

CONFIDENTIAL

CONFIDENTIAL

NPG REPORT NO. 1211

TABLE XIV (Continued)

Projectile	Plate Number	Plate Tensile Strength	θ	$\frac{e}{d}$	Uncorrected $F(\frac{e}{d}, \theta)$
3" AP Expr Mk 29 (flat nose + Ws)	40917	124000	30°	.489	39700 ± 200
3" AP Expr Mk 29 (flat nose + Ws)	40917	124000	45°	.501	41500 ± 600
3" AP Expr Mk 29 (flat nose + Ws)	40917	124000	60°	.500	41500 ± 900
3" AP Type A + cap	54986	126000	30°	.402	45400 ± 200
37mm AP M51B2 + cap	55909	118000	0°	.835	52200 ± 200
37mm AP M51B2 - cap	55909	118000	0°	.835	47900 ± 300
3" AP Type A + cap	55909	118000	3°	.406	43800 ± 500
3" AP Type A - cap	55909	118000	2°	.407	38800 ± 200
3" AP Type A - cap	55909	118000	8°	.409	44000 ± 1000
3" AP Type A + cap	55909	119000	29°	.404	44000 ± 500
3" AP Type A + cap	55909	118000	30°	.409	43000 ± 200
3" AP Type A + $\frac{1}{2}$ cap	55909	118000	30.5°	.409	40800 ± 200
3" AP Type A - cap	55909	119000	32°	.406	35600 ± 300
3" AP Type A + cap	55909	119000	45°	.408	39100 ± 200
3" AP Type A - cap	55909	119000	45°	.408	35000 ± 500
3" AP Type A + cap	55909	120000	50.5°	.411	38500 ± 800
3" AP Type A - cap	55909	120000	50°	.411	37300 ± 1000

CONFIDENTIAL

CONFIDENTIAL

NPG REPORT NO. 1211

TABLE XIV (Continued)

Projectile	Plate Number	Plate Tensile Strength	θ	$\frac{e}{d}$	$F(\frac{e}{d}, \theta)$
3" AP Type A + cap	55909	119000	60°	.409	39000 ± 1000
3" AP Type A - cap	55909	119000	59.5°	.409	≥48500
3" AP M61 + standard cap RC = 49	55909	119000	30°	.435	43500 ± 500
3" AP M61 + soft cap RC = 33	55909	119000	30°	.435	45000 ± 800
37mm AP M51B2 + cap	56360	123000	30°	.433	41600 ± 500
37mm AP M51B2 - cap	56360	123000	31°	.433	38500 ± 500
37mm AP M51B2 + cap	60919	122000	3°	.447	50200 ± 500
37mm AP M51B2 - cap	60919	122000	2°	.445	47800 ± 200
37mm AP M51B2 + cap	60919	122000	30°	.448	49200 ± 300
37mm AP M51B1 - cap	60919	122000	29.5°	.444	41800 ± 500
3" AP Type A + cap	60919	122000	5°	.217	35800 ± 200
3" AP Type A - cap	60919	124000	10°	.212	34000 ± 500
3" AP Type A + cap	60919	122000	30°	.219	32400 ± 200
3" AP Type A + cap	60919	122000	31°	.218	32100 ± 200
3" AP Type A + cap	60919	122000	31°	.211	30400 ± 200
3" AP Type A - cap	60919	122000	31°	.213	30500 ± 500

CONFIDENTIAL

TABLE XIV (Continued)

Projectile	Plate Number	Plate Tensile Strength	θ	$\frac{e}{d}$	Uncorrected $F(\frac{e}{d}, \theta)$
3" AP Type A + cap	60919	124000	46°	.211	32000 ± 200
3" AP Type A + cap	60919	122000	50°	.214	33500 ± 500
3" AP Type A - cap	60919	122000	52°	.210	34000 ± 1000
3" AP Type A - cap	60919	124000	59°	.215	≥34000
3" AP M62 BS	70015	118000	30°	.237	33500 ± 500
37mm AP M51B2 + cap	83880	122000	0°	.503	50200 ± 300
37mm AP M51B2 - cap	83880	122000	4°	.504	48900 ± 200
37mm AP M51B2 + cap	83880	122000	30.5°	.503	49700 ± 300
37mm AP M51B2 - cap	83880	122000	30.5°	.504	45300 ± 500
3" AP Mk 29-2	85187	126000	.5°	1.023	56500 ± 500
3" AP Mk 29-2	85187	126000	20°	1.022	56500 ± 300
3" AP Mk 29-2	85187	126000	30°	1.023	55900 ± 600
3" AP Mk 29-2	85187	126000	34.8°	1.023	56600 ± 400
3" AP Type A + cap	87207	125000	1°	.819	50000 ± 500
3" AP Type A - cap	87207	125000	1°	.819	45000 ± 500
3" AP Type A + cap	87207	125000	30°	.819	47500 ± 500
3" AP Type A-1 - cap	87207	125000	28.5°	.819	45000 ± 500
3" AP Mk 29-2 OLDS	87207	125000	30°	.813	50900 ± 300
3" AP Type A + cap	87207	112000	2°	.813	52000 ± 200
3" AP Type A + cap	87207	112000	30°	.807	49800 ± 200

CONFIDENTIAL

TABLE XIV (Continued)

Projectile	Plate Number	Plate Tensile Strength	θ	$\frac{e}{d}$	Uncorrected $F(\frac{e}{d}, \theta)$
3" AP Mk 29-1	87547	128000	40°	.654	52900 ± 500
3" AP Mk 29A	87547	128000	40°	.653	53900 ± 300
3" AP Mk 29B	87547	128000	39.5°	.652	49500 ± 500
3" AP Mk 29C	87547	128000	40°	.652	49000 ± 1000
3" AP M62 BS	88521	106000	0°	.799	55000 ± 300
3" AP M62 BS	88521	106000	20°	.799	53400 ± 300
3" AP M62 BS	88521	106000	30°	.802	50400 ± 400
3" AP M62 BS	88521	106000	40°	.802	48600 ± 600
3" AP M62 BS*	88521	106000	50°	.799	55000 ± 900
3" AP M62 CHEV	88521	115000	20°	.791	56600 ± 1200
3" AP M62 CHEV	88521	115000	30°	.793	50800 ± 600
3" AP M62 CHEV	88521	115000	40°	.793	49600 ± 1400
3" AP Type A + cap	89001-A7	114000	0°	1.006	54000 ± 200
3" AP Type A + cap	89001-A7	114000	30°	1.00	53000 ± 500
3" AP M61	89001-A7	114000	29.5°	1.006	52800 ± 500
3" AP M61	89002-A	114000	30°	.995	53500 ± 200
3" AP M61	89004-A1	114000	29.7°	.997	54250 ± 100
37mm AP M51B2 + cap	90940-A1	91000	1°	1.367	55600 ± 200
37mm AP M51B2 + cap	90940-A	111000	1°	1.365	57300 ± 700
37mm AP M51B2 + cap	90940-A2	114000	0°	1.369	57600 ± 200

* Broken Projectile

CONFIDENTIAL

CONFIDENTIAL

NPG REPORT NO. 1211

TABLE XIV (Continued)

Projectile	Plate Number	Plate Tensile Strength	θ	$\frac{e}{d}$	Uncorrected $F(\frac{e}{d}, \theta)$
3" AP Type A	96746		35°	.494	43000 ± 300
37mm AP M51B2 + cap NL	98193	116000	2°	1.362	58600 ± 300
37mm AP M51B2 - cap NL	98193	116000	1°	1.367	53300 ± 300
3" AP M62 CHEV	98193	116000	29.8°	.659	51700 ± 700
37mm AP M51B2 + cap* NL	98193	126000	1°	1.352	≥ 60000
37mm AP M51B2 - cap NL	98193	126000	1°	1.352	54300 ± 200
3" AP M62 CHEV	98193	126000	30°	.654	51900 ± 1000
37mm AP M51B2 + cap	103103	113000	2°	.508	51300 ± 800
37mm AP M51B2 - cap	103103	113000	2°	.510	48300 ± 200
37mm AP M51B2 + cap	103103	113000	30°	.507	49700 ± 1000
37mm AP M51B2 - cap	103103	113000	30°	.509	45400 ± 800
37mm AP M51B2 + cap	103103	128000	2°	.505	52300 ± 700
37mm AP M51B2 - cap	103103	128000	2.5°	.506	49700 ± 600
37mm AP M51B2 + cap	103103	128000	30°	.510	49600 ± 500
37mm AP M51B2 + cap	107238	119000	1°	.940	54700 ± 100
37mm AP M51B2 - cap	107238	119000	1°	.944	50800 ± 300

* Broken Projectile

CONFIDENTIAL

CONFIDENTIAL

NPG REPORT NO. 1211

TABLE XIV (Continued)

Projectile	Plate Number	Plate Tensile Strength	θ	$\frac{e}{d}$	Uncorrected $F(-\frac{e}{d}, \theta)$
3" AP M61 BS	107238	119000	35°	.461	46700 ± 300
3" AP Type A	114400		29°	.640	48000 ± 300
3" AP M61	127804-A1	114000	30°	1.013	52300
3" AP Type A + cap	131939	121000	34.5°	.356	40500 ± 500
3" AP Type A - cap	131939	121000	36°	.356	35700 ± 1000
37mm AP M51B2 + cap	148939	132000	5°	1.374	59000 ± 400
37mm AP M51B2 - cap	148939	132000	5°	1.375	55000 ± 800
3" AP M62 CHEV	148939	132000	30°	.669	48900 ± 1100
37mm AP M51B2 + cap	149950	139000	2°	1.372	60300 ± 300
37mm AP M51B2 - cap	149950	139000	2°	1.376	59400 ± 200
3" AP M62 CHEV	149950	139000	30°	.665	51500 ± 700
37mm AP M51B2 + cap	161855	118000	2°	.542	51600 ± 200
37mm AP M51B2 - cap	161855	118000	3°	.541	46500 ± 200
37mm AP M51B2 + cap	161855	118000	30°	.539	47500 ± 300
37mm AP M51B2 - cap	161855	118000	30°	.540	42000 ± 800

CONFIDENTIAL

CONFIDENTIAL

NPG REPORT NO. 1211

TABLE XIV (Continued)

Projectile	Plate Number	Plate Tensile Strength	θ	$\frac{e}{d}$	Uncorrected $F(\frac{e}{d}, \theta)$
3" AP Type A + cap	161855	118000	1.5°	.262	37400 ± 200
3" AP Type A - cap	161855	118000	8°	.259	33800 ± 200
3" AP Type A + cap	161855	119000	31°	.259	33600 ± 200
3" AP Type A - cap	161855	119000	28.5°	.260	33500 ± 500
3" AP Type A + cap	161855	118000	46°	.261	33500 ± 800
3" AP Type A - cap	161855	118000	44.5°	.263	31500 ± 1000
3" AP Type A + cap	161855*	119000	60°	.264	35800 ± 800
3" AP Type A + cap	161855**	119000	60°	.263	35800 ± 800
3" AP Type A - cap	161855*	119000	60°	.261	37000 ± 500
3" AP Type A - cap	161855**	119000	59°	.262	37000 ± 1000
3" AP M62 BS	174140	118000	30.2°	.358	37400 ± 300
3" AP Mk 29-2	174140	118000	1°	.357	42800 ± 300
3" AP Mk 29-2	174140	118000	30°	.362	43700 ± 700
3" AP Mk 29-2	174140	118000	45.2°	.357	42600 ± 200
3" AP Mk 29-2	174140	118000	60.5°	.362	46900 ± 400
3" AP Expr Mk 29 (flat nose + Ws)	174140	118000	1°	.358	37400 ± 300

* Trajectory along the direction of rolling in the plate

** Trajectory across the direction of rolling in the plate

CONFIDENTIAL

CONFIDENTIAL

TABLE XIV (Continued)

Projectile	Plate Number	Plate Tensile Strength	θ	$\frac{e}{d}$	Uncorrected $F(\frac{e}{d}, \theta)$
3" AP Expr Mk 29 (flat nose + Ws)	174140	118000	30°	.362	33200 ± 1000
3" AP Expr Mk 29 (flat nose + Ws)	174140	118000	45°	.357	31500 ± 300
3" AP Expr Mk 29 (flat nose + Ws)	174140	118000	60.2°	.361	32800 ± 500
3" AP M62 BS	179770	108000	0°	1.010	55000 ± 300
3" AP M62 BS	179770	108000	20°	1.014	54200 ± 200
3" AP M62 BS	179770	108000	30°	1.011	53000 ± 100
3" AP M62 BS	179770	107000	40°	1.012	52100 ± 400
3" AP M62 BS	179770	107000	45°	1.010	55000 ± 900
3" AP M62 CHEV	179770	109000	20°	1.016	54200 ± 300
3" AP M62 CHEV	179770	109000	30°	1.015	52600 ± 200
3" AP Mk 29-2	179770	109000	30°	1.011	57000 ± 300
3" AP Mk 29-2	179770	109000	40°	1.011	56200 ± 200
3" AP Mk 29-2	187609	123000	29°	.661	53500 ± 400
3" AP M62 BS	612068	108000	.5°	.162	30000 ± 200
3" AP M62 BS	612068	108000	20°	.163	27500
3" AP M62 BS	612068	108000	30°	.163	27300 ± 200

CONFIDENTIAL

CONFIDENTIAL

NPG REPORT NO. 1211

TABLE XIV (Continued)

Projectile	Plate Number	Plate Tensile Strength	θ	$\frac{e}{d}$	Uncorrected $F(\frac{e}{d}, \theta)$
3" AP M62 BS	612068	108000	40°	.163	27000 ± 200
3" AP M62 BS	612068	108000	50°	.163	30300 ± 600
3" AP M62 BS	612068	108000	60°	.163	29800 ± 300
3" AP M61	694385	130000	30°	.245	35600 ± 200
3" AP Dw DA302-HC (A-1+Mk 11 cap)	694385	130000	30°	.244	32800 ± 200
3" AP Dw DA302-SC (A-1+Mk 11 cap)	694385	130000	30°	.243	≥ 37000
3" AP Dw DA303 (A-1+ light cap)	694385	130000	30°	.243	≥ 24400
3" AP Dw DA304 (A-1+ heavy cap)	694385	130000	29.5°	.244	35500 ± 200
3" AP Dw 3001 (Mk 11-1)	694385	130000	30.5°	.243	34500 ± 200
3" AP Type A-1	694385	130000	60°	.245	40100 ± 1800
3" AP M61	694385	130000	60°	.246	37500 ± 600
3" AP Dw DA302-HC (A-1+ Mk 11 cap)	694385	130000	60°	.246	36500 ± 2500

CONFIDENTIAL

CONFIDENTIAL

TABLE XIV (Continued)

Projectile	Plate Number	Plate Tensile Strength	θ	$\frac{e}{d}$	Uncorrected $F(\frac{e}{d}, \theta)$
3" AP Dw DA302-SC (A-1+ Mk 11 cap)	694385	130000	60°	.246	≤ 43600
3" AP Dw DA303 (A-1+ light cap)	694385	130000	60°	.245	41700 \pm 400
3" AP Dw DA304 (A-1+ heavy cap)	694385	130000	60°	.244	40500 \pm 1500
3" AP Dw 3001 (Mk 11-1)	694385	130000	60°	.246	≥ 42100
3" AP Mk 29-1	694385	130000	60°	.247	≥ 37300
3" AP M62 BS	F1790	115000	20°	.663	51500 \pm 400
3" AP M62 BS	F1790	115000	30.5°	.663	49600 \pm 800
3" AP Mk 29-2	F1790	115000	.5°	.663	57500 \pm 500
3" AP Mk 29-2	F1790	115000	30°	.659	52000 \pm 200
3" AP Mk 29-2	F1790	115000	45°	.663	52500 \pm 200
3" AP Expr Mk 29 (flat nose + Ws)	F1790	115000	.5°	.661	≥ 44000
3" AP Expr Mk 29 (flat nose + Ws)	F1790	115000	30°	.660	42600 \pm 1000

CONFIDENTIAL

CONFIDENTIAL

NPG REPORT NO. 1211

TABLE XIV (Continued)

Projectile	Plate Number	Plate Tensile Strength	θ	$\frac{e}{d}$	Uncorrected $F(\frac{e}{d}, \theta)$
3" AP Expr Mk 29* (flat nose + ws)	F1790	115000	45°	.662	49700 ± 500
3" AP M62 BS	F3076	112000	0°	.653	54800 ± 200
3" AP M62 BS	F3076	112000	20°	.656	52700 ± 200
3" AP M62 BS	F3076	112000	30°	.654	50700 ± 500
3" AP M62 BS	F3076	112000	40°	.653	48400 ± 200
3" AP M62 BS	F3076	112000	45°	.654	53200 ± 300
3" AP M62 BS*	F3076	113000	50°	.652	≤49300
3" AP M62 BS	F3076	96000	50°	.649	≥47400
3" AP M62 BS	F3076	96000	60°	.649	≥53000
37mm AP M51B2 + cap	08451	106000	1°	.827	53500 ± 500
37mm AP M51B2 - cap	08451	106000	1°	.827	48900 ± 200
37mm AP M51B2 + cap*	08451	106000	30°	.827	≤50200
37mm AP M51B2 + cap	08451	125000	2°	.827	54400 ± 400
37mm AP M51B2 - cap	08451	125000	2°	.827	50200 ± 300
37mm AP M51B2 + cap	08451	125000	30°	.827	52400 ± 300
3" AP M62 BS	017784	114000	0.5°	.334	37100 ± 200
3" AP M62 BS	017784	114000	20°	.334	41800 ± 200

* Broken Projectile

CONFIDENTIAL

TABLE XIV (Continued)

Projectile	Plate Number	Plate Tensile Strength	θ	$\frac{e}{d}$	Uncorrected $F(\frac{e}{d}, \theta)$
3" AP M62 BS	017784	111000	30°	.332	35700 ± 200
3" AP M62 BS	017784	113000	40°	.337	38400 ± 800
3" AP M62 BS	017784	112000	50°	.336	39100 ± 800
3" AP M62 BS	017784	113000	60°	.336	43900 ± 900
3" AP M79	017784	113000	30°	.333	37200 ± 300
3" AP Type A-1	X9021	120000	.5°	1.072	54000 ± 500
3" AP M61	X9021	120000	.5°	1.076	58200 ± 200
3" AP M61	X9021	120000	30°	1.065	55200 ± 700
3" AP Dw DA302-HC (A-1+ Mk 11 cap)	X9021	120000	.5°	1.069	54900 ± 300
3" AP Dw DA302-SC (A-1+ Mk 11 cap)	X9021	120000	0°	1.070	55000 ± 300
3" AP Dw DA304 (A-1+ heavy cap)	X9021	120000	0°	1.069	55900 ± 800
3" AP Dw 3001 (Mk 11-1)	X9021	120000	0°	1.070	52300 ± 300
3" AP Mk 29-1	X9021	120000	0°	1.070	57500 ± 500
3" AP Type A-1	XL2904	122000	.5°	.651	52000 ± 500

CONFIDENTIAL

NPG REPORT NO. 1211

TABLE XIV (Continued)

Projectile	Plate Number	Plate Tensile Strength	θ	$\frac{e}{d}$	Uncorrected $F(\frac{e}{d}, \theta)$
3" AP M61	XL2904	122000	2°	.651	53700 ± 300
3" AP Dw DA302-HC (A-1 + Mk 11 cap)	XL2904	122000	4°	.650	51800 ± 500
3" AP Dw DA302-SC (A-1 + Mk 11 cap)	XL2904	122000	1°	.651	50600 ± 500
3" AP Dw DA303 (A-1 + light cap)	XL2904	122000	4.5°	.650	51700 ± 500
3" AP Dw DA304 (A-1 + heavy cap)	XL2904	122000	1.5°	.651	53600 ± 200
3" AP Dw 3001 (Mk 11-1)	XL2904	122000	3°	.650	50200 ± 500
3" AP Type A-1	XL2904	122000	30.5°	.652	49000 ± 300
3" AP M61	XL2904	122000	29.5°	.651	50600 ± 200
3" AP Dw DA302-HC (A-1 + Mk 11 cap)	XL2904	122000	30°	.650	45400 ± 500
3" AP Dw DA302-SC (A-1 + Mk 11 cap)	XL2904	122000	30°	.650	47300 ± 300

CONFIDENTIAL

CONFIDENTIAL

TABLE XIV (Continued)

Projectile	Plate Number	Plate Tensile Strength	θ	$\frac{e}{d}$	Uncorrected $F(\frac{e}{d}, \theta)$
3" AP Dw DA303 (A-1 + light cap)	XL2904	122000	30°	.652	47800 ± 300
3" AP Dw DA304 (A-1 + heavy cap)	XL2904	122000	30°	.652	50200 ± 300
3" AP Dw 3001 (Mk 11-1)	XL2904	122000	29.5°	.650	43600 ± 800
3" AP M62	XL2904	122000	45°	.648	50100 ± 500
3" AP Mk 29A	XL2904	122000	30°	.650	50600 ± 300
3" AP Mk 29B	XL2904	122000	30°	.650	54000 ± 500
3" AP Mk 29C	XL2904	122000	30°	.652	50000 ± 200
3" AP Mk 29-1	XL2904	122000	30°	.651	52100 ± 200
3" AP Mk 29-2 OLDS	XL2904	122000	40°	.648	48000 ± 600
3" AP M62 BS	XL8305	107000	1°	.675	52000 ± 500
3" AP M62 BS	XL8305	107000	29.8°	.675	49500 ± 800
3" AP M62 BS	XL8305	107000	45°	.673	48300 ± 700
3" AP Mk 29-1	XL8305	121000	1.5°	.676	54800 ± 200
3" AP M62 BS	DD36	111000	0°	1.408	56800 ± 300
3" AP M62 BS	DD36	111000	20°	1.386	57100 ± 200
3" AP M62 BS	DD36	111000	30°	1.40	55300 ± 200

CONFIDENTIAL

TABLE XIV (Continued)

Projectile	Plate Number	Plate Tensile Strength	θ	$\frac{e}{d}$	Uncorrected $F(\frac{e}{d}, \theta)$
3" AP M62 BS	DD36	111000	35°	1.402	56100 ± 300
3" AP Mk 29-1	DD36	111000	0°	1.463	61000 ± 200
3" AP Mk 29A	DD36	111000	1°	1.443	60700 ± 100
3" AP Mk 29B	DD36	111000	1°	1.426	61300 ± 200
3" AP Mk 29C	DD36	111000	1°	1.422	60800 ± 200
3" AP Type A + cap	DD37	108000	.5°	1.376	53500 ± 1000
3" AP M61 + standard cap RC = 49	DD37	108000	0°	1.37	57300 ± 500
3" AP M61 + soft cap RC = 33	DD37	108000	0°	1.37	57900 ± 100
3" AP M62 BS	DD37	109000	30°	1.374	54000 ± 800
3" AP M62 BS	DD37	127000	30°	1.358	57700 ± 500
3" AP M62 BS	DD37	135000	30°	1.365	57100 ± 1000
3" AP M62 CHEV	DD37	109000	20°	1.403	59500 ± 700
3" AP Mk 29-1	DD37	108000	0°	1.36	58800 ± 500
3" AP Mk 29-2	DD37	109000	30°	1.375	60000 ± 300

CONFIDENTIAL

TABLE XIV (Continued)

Projectile	Plate Number	Plate Tensile Strength	θ	$\frac{e}{d}$	Uncorrected $F(\frac{e}{d}, \theta)$
3" AP Type A + cap	DD318	109000	1°	.953	52500 ± 1000
3" AP Type A - cap	DD318	109000	1.5°	.980	45500 ± 200
3" AP Type A + cap	DD318	109000	31°	.973	51500 ± 1000
3" AP Type A-1	DD319	110000	1.5°	1.433	53100 ± 200
3" AP Type A + cap	DD804	109000	0°	1.067	54300 ± 200
3" AP Type A + cap	DD804	109000	30°	1.067	53500 ± 300
3" AP M61 - Ws	GG125	116000	1°	1.621	58300 ± 200
3" AP M61 - Ws	GG125	116000	30°	1.621	54000 ± 1000
3" AP M62 BS	GG125	116000	1.6°	1.646	61100 ± 600
3" AP M62 BS	GG125	116000	20°	1.640	59500 ± 700
37mm AP M51B2 + cap	GG296	97000	3°	1.69	57200 ± 300
37mm AP M51B2 - cap	GG296	97000	4.5°	1.69	52300 ± 300
3" AP Type A + cap	GG296	97000	30.5°	.823	48800 ± 200
3" AP Type A + cap	GG296	103000	29.5°	.826	49900 ± 500
3" AP Type A + cap	GG296	111000	30°	.826	49000 ± 500
3" AP M61	GG346 ¹ / ₈	117000	29.5°	1.033	56500 ± 300
3" AP Type A + cap	HH135	121000	1°	1.02	54800 ± 800

CONFIDENTIAL

CONFIDENTIAL

NPG REPORT NO. 1211

TABLE XIV (Continued)

Projectile	Plate Number	Plate Tensile Strength	θ	$\frac{e}{d}$	Uncorrected $F(\frac{e}{d}, \theta)$
3" AP Type A - cap	HH135	121000	1°	1.02	50000 ± 1000
3" AP Type A + cap	HH135	121000	31°	1.02	54000 ± 1000
3" AP Type A + cap	HH161	125000	0°	.986	54700 ± 200
3" AP Mk 29-1 + cap	HH161	127000	20°	.987	58300 ± 200
37mm AP M51B2 + cap	HH514*	105000	.5°	.753	54900 ± 200
37mm AP M51B2 + cap	HH514**	105000	1°	.757	54600 ± 200
3" AP Type A-1	2A555A1	100000	16.5°	1.666	53800 ± 300
3" AP Type A	5A779A1	107000	3°	1.69	51800 ± 1000
37mm AP M51B2 + cap	53E246A8	116000	1°	1.369	58300 ± 500
3" AP M62 CHEV	53E246A8	116000	30°	.662	50000 ± 400
37mm AP M51B2 + cap	53E246A7	127000	1°	1.380	60700 ± 1000
37mm AP M51B2 + cap	53E246A2	127000	1°	1.370	60500 ± 200
3" AP M62 CHEV	53E246A8	127000	30°	.666	52900 ± 300
3" AP M62 CHEV	53E246A2	127000	30°	.665	51100 ± 300

* Section from center of 10.6" plate

** Section from surface of 10.6" plate

CONFIDENTIAL

TABLE XV

Armor and Projectile Laboratory data on the decapping of AP Projectiles by STS Plates

Projectile	θ	$\frac{e}{d}$	Cap Condition	Record
37mm AP M51B2	30°	.50	shattered	X-ray
"	"	.26	decapped	X-ray
"	"	.17	"	"
"	60°	.51	shattered	X-ray
"	75°	.176	decapped	X-ray
3" AP M62	0°	.510	decapped	fragments
"	"	.334	decapped	"
"	"	.162	intact	"
"	20°	.495	shattered	scars
"	"	.334	decapped	fragments
"	"	.163	intact	"
"	30°	.497	shattered	"
"	"	.333	decapped	"
"	"	.237	decapped	"
"	"	.163	intact	"
"	40°	.500	shattered	"
"	"	.337	decapped	"
"	"	.163	intact	"
"	50°	.498	shattered	"
"	"	.335	decapped	"
"	"	.163	decapped*	"
"	60°	.496	shattered	scars
"	"	.336	shattered	fragments
"	"	.163	decapped	"
3" AP Mk 29-2	0°	.165	decapped*	"
"	"	.125	intact**	"
"	"	.086	intact	"
"	30°	.206	decapped**	"
"	"	.165	intact	"
"	"	.165	decapped**	"
"	"	.126	intact**	"
"	45°	.165	decapped*	"
"	"	.124	decapped**	"
"	60°	.164	decapped	"

* Incomplete penetrations only

** High velocity impact

TABLE XVI

Plate Battery Data on the Decapping of Projectiles by STS Plates

Projectile	θ	$\frac{e}{d}$	Cap Condition	Record
6" AP Mk 35-5	30°	.527	decapped	stuck in plate
standard cap	"	.428	broken	yaw card
"	"	.373	broken	"
"	"	.328	decapped	"
"	"	.243	decapped	"
"	"	.203	decapped	"
"	"	.160	decapped	"
"	"	.125	decapped	"
"	"	.120	decapped	"
"	"	.083	decapped	"
"	"	.080	intact	"
"	"	.062	intact	"
"	40°	.492	decapped	stuck in plate
"	45°	.082	decapped	yaw card
"	"	.080	intact	"
"	"	.062	intact	"
"	60°	.080	decapped	"
"	"	.062	intact	"
set screw cap	30°	.178	decapped	"
"	"	.125	intact	"
8" AP Mk 21-1	30°	.156	broken*	motion picture
"	"	.124	decapped	"
"	"	.094	decapped	"
8" AP Mk 19-1	40°	.305	decapped	fragments
8" AP Mk 19-4	40°	.300	decapped	stuck in plate
8" AP Mk 20-4	50°	.469	shattered	fragments
8" AP Mk 19-Expr.	50°	.380	decapped	fragments
8" AP Type H	50°	.368	decapped	fragments

* Cap broke up after penetration of plate

APPENDIX E

LIST OF SYMBOLS

a	swell radius of an ogive at the circle of tangency.
b	distance from the circle of tangency to the tip of an ogive.
C	transverse moment of inertia of the body.
d	diameter of the projectile.
e	thickness of the plate.
f_1	longitudinal component of force on the body.
f_2	transverse component of force on the body.
$F(e/d, \theta)$	plate penetration coefficient.
F_s	impact parameter.
F_R	residual velocity function.
h	thickness of the crown before deformation.
h'	thickness of the crown after deformation.
h'_0	dimensionless parameter which is proportional to the plate penetration coefficient.
i, j, k	orthogonal unit vectors with k perpendicular to the plate and with i perpendicular to the plane of incidence.
L	torque on the body.
m	whole mass of the projectile.
m_0	mass of the body.
m_1	mass of the windshield.
m_2	mass of the hood.
m_3	mass of the cap.
M	bending moment.

n	unit vector normal to the ogive.
p	penetration of the tip of an ogive into a plane of intersection.
r, φ, z	cylindrical polar coordinates of a point on the nose contour.
R	arc radius of an ogive.
ρ	density.
s	surface area of an ogive.
t	unit vector tangent to the ogive.
θ	angle of obliquity between the velocity of the body and the normal of the plate.
$\Delta\theta$	angle of rotation of the velocity of the body.
θ_1	parameter of the windshield effect.
θ_2	parameter of the hood effect.
u	parameter of the torque on the body.
$U(e/d, \theta)$	limit energy function.
v	particle velocity.
v_L	limit velocity.
v_s	striking velocity.
$\Delta\omega$	increment of kinetic energy of the body.
x, y	cartesian coordinates of the contour of a plane cross section through an ogive.
X'_0	yield stress of the plate.
X'_1	yield stress of the hood.
χ	angle of orientation between the axis of the projectile and the normal of the plate.

χ_0 initial angle of orientation.
 $\Delta\chi$ angle of rotation of the axis of the body.
 $\dot{\Delta\chi}$ angular velocity of the axis of the body.
 χ_0' dimensionless parameter which is proportional to the initial rate of yaw.

APPENDIX F

BIBLIOGRAPHY

- (1) "The Speed of Propagation of Brittle Cracks in Steel," G. Hudson and M. Greenfield, J. App. Phys. 18 405 (1947)
- (2) "The Brittle Failure of Medium Steel in Ship Structures," W. P. Roop, DTMB Report No. R-207 (Oct. 1943); "Notes on The Conditions of Brittle Rupture of Ship Plates of Medium Steel," W. P. Roop, DTMB Report No. R-276 (July 1944); "Additional Notes on the Conditions of Fracture of Medium Steel Ship Plates," D. F. Windenburg and W. P. Roop, DTMB Report No. R-271 (June 1945)
- (3) "Velocity Loss of a 1/2-Inch Model Projectile When It Penetrates 1/32-Inch Cold-Rolled Sheet Steel," G. D. Kinzer and A. C. Jantzen, NRL Report No. O-2263 (Mar. 1944); "Penetration of Thin Hot-Rolled Steel by 37mm Model Projectile," P. Beij, NRL Report No. O-2891 (Aug. 1946)
- (4) "The Penetration of Homogeneous Light Armor by Jacketed Projectiles at Normal Obliquity," NPG Report No. 14-43 (July 1943)
- (5) "The Effect of Cap Design on 3-Inch Projectile Performance," NPG Report No. 16-43 (Dec. 1943)
- (6) "Penetration of Homogeneous Plate of One Tensile Strength (110 000 psi) by 3" Capped M62 AP Projectiles," NPG Report No. 6-45 (May 1945)
- (7) "Effect of Plate Tensile Strength on the Ballistic Limits of 2" Homogeneous Armor of Four Different Compositions Against 37mm Capped AP, 3" M62 Capped AP, and 3" M79 Monobloc SAP Projectiles," NPG Report No. 9-45 (June 1945)
- (8) "A Study of Non-Uniformity in 3" and 4" Homogeneous Armor," NPG Report No. 11-46 (July 1946)
- (9) "Perforation Limits for Nonshattering Projectile Against Thick Homogeneous Armor at Normal Incidence," C. W. Curtis and R. L. Kramer, NDRC Report No. A-393 (Dec. 1945); "Effect of Armor Piercing Cap on Perforation Limits," C. W. Curtis and R. J. Emrich, NDRC Monthly Report OTB-10g (May 15, 1945)

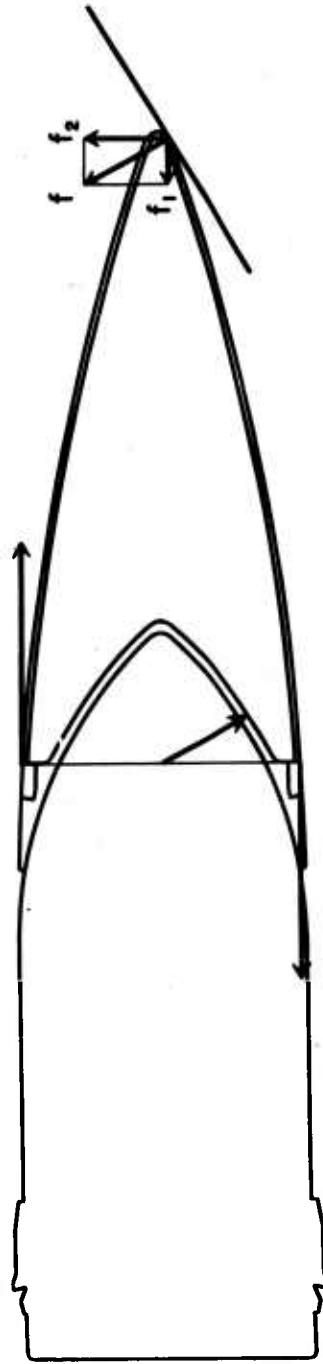
BIBLIOGRAPHY (Continued)

- (10) "Analytical Summary Part III. Plastic Flow in Armor Plate," NPG Report No. 864
- (11) "Analytical Summary Part V. Plastic Flow in Bars and Shells," NPG Report No. 954
- (12) "Analytical Summary Part VI. The Theory of Projectile Ricochet," NPG Report No. 1041

APPENDIX G

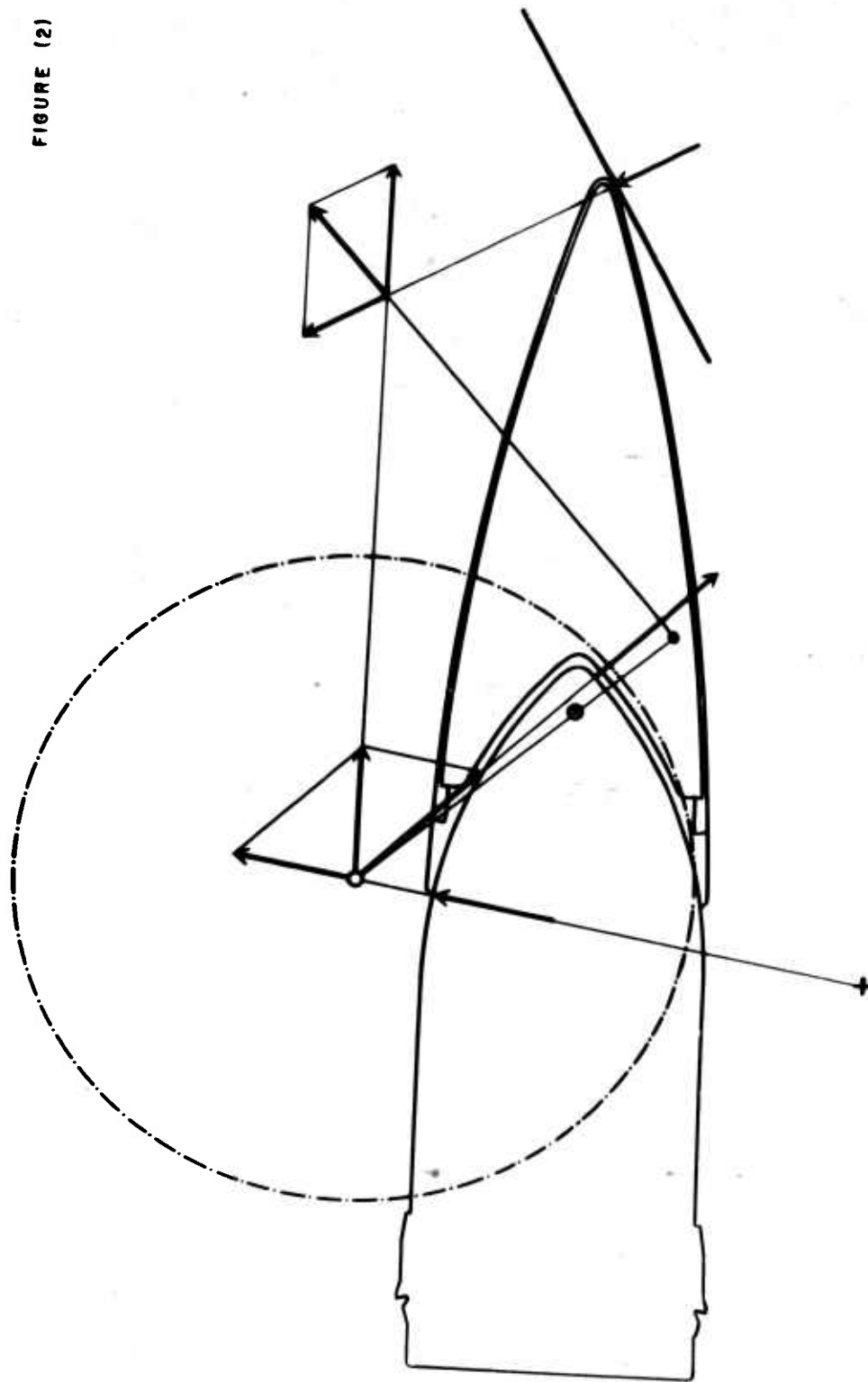
FIGURE (1)

NP9 49383



SCHEMATIC DIAGRAM TO ILLUSTRATE THE FORCES AND TORQUE ON THE WINDSHIELD
BEFORE THE WINDSHIELD BEGINS TO YIELD AT THE BASE

FIGURE (2)



SCHEMATIC DIAGRAM TO ILLUSTRATE THE PIVOT REACTION ON THE HOOD WHEN THE
HOOD AND WINDSHIELD MOVE TOGETHER AS A SINGLE UNIT

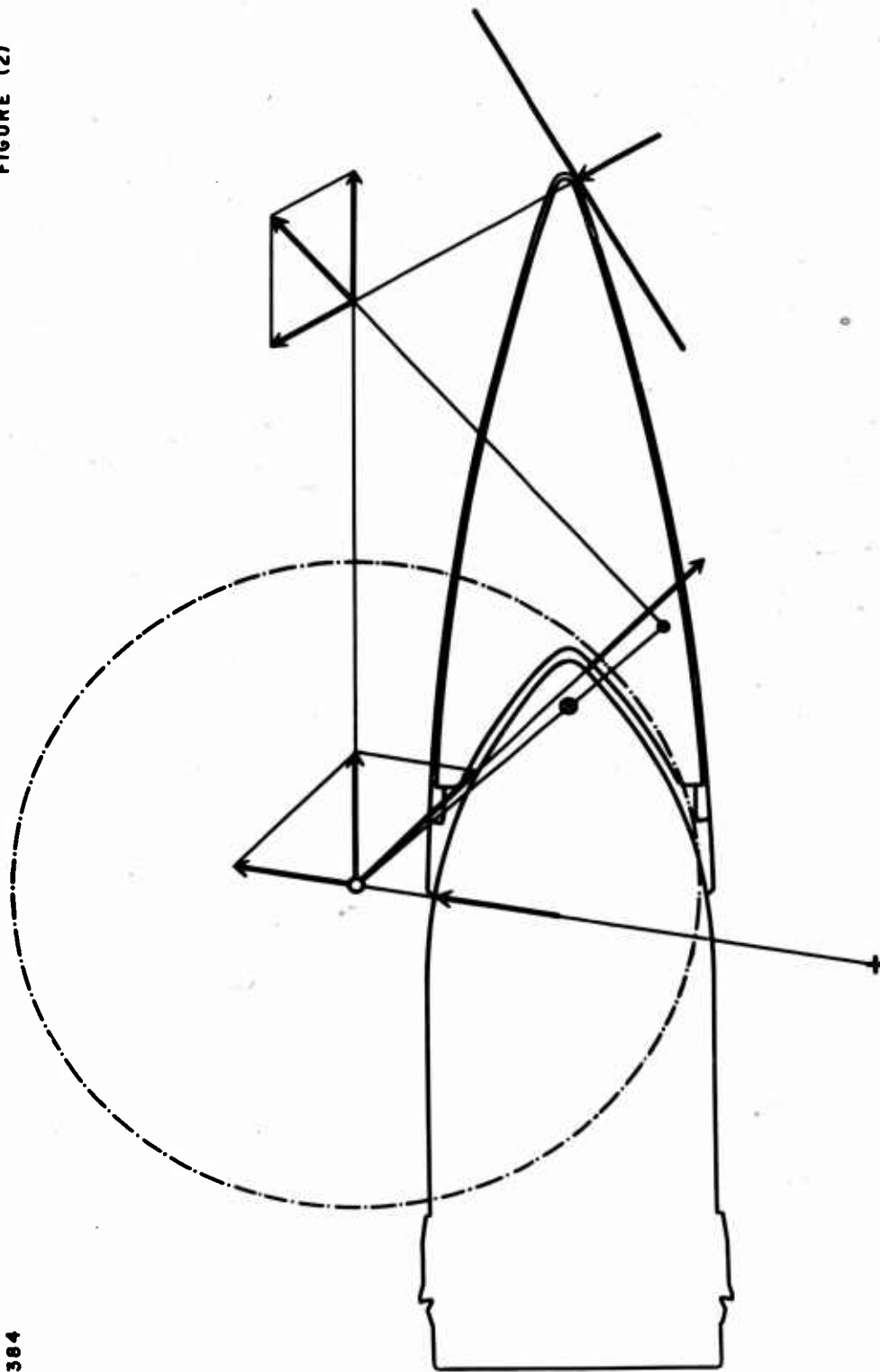
Center of ogival arc
Center of percussion

○ Pivot

⊙ Center of mass
--- Radius of gyration

NP9 49384

FIGURE (2)

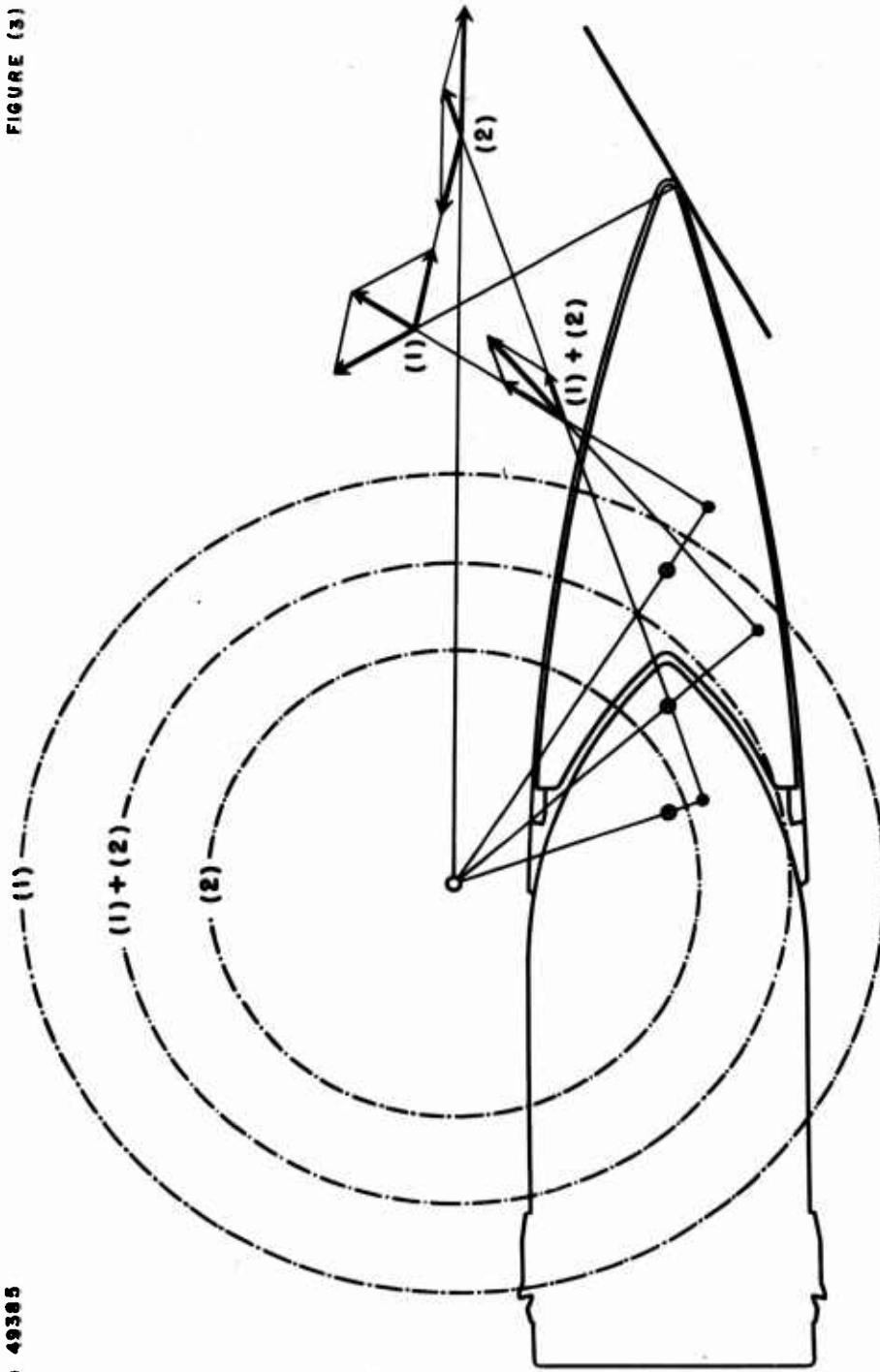


SCHEMATIC DIAGRAM TO ILLUSTRATE THE PIVOT REACTION ON THE HOOD WHEN THE HOOD AND WINDSHIELD MOVE TOGETHER AS A SINGLE UNIT

- + Center of ogival arc
- Center of percussion
- Pivot
- ⊙ Center of mass
- Radius of gyration

NP9 49385

FIGURE (3)

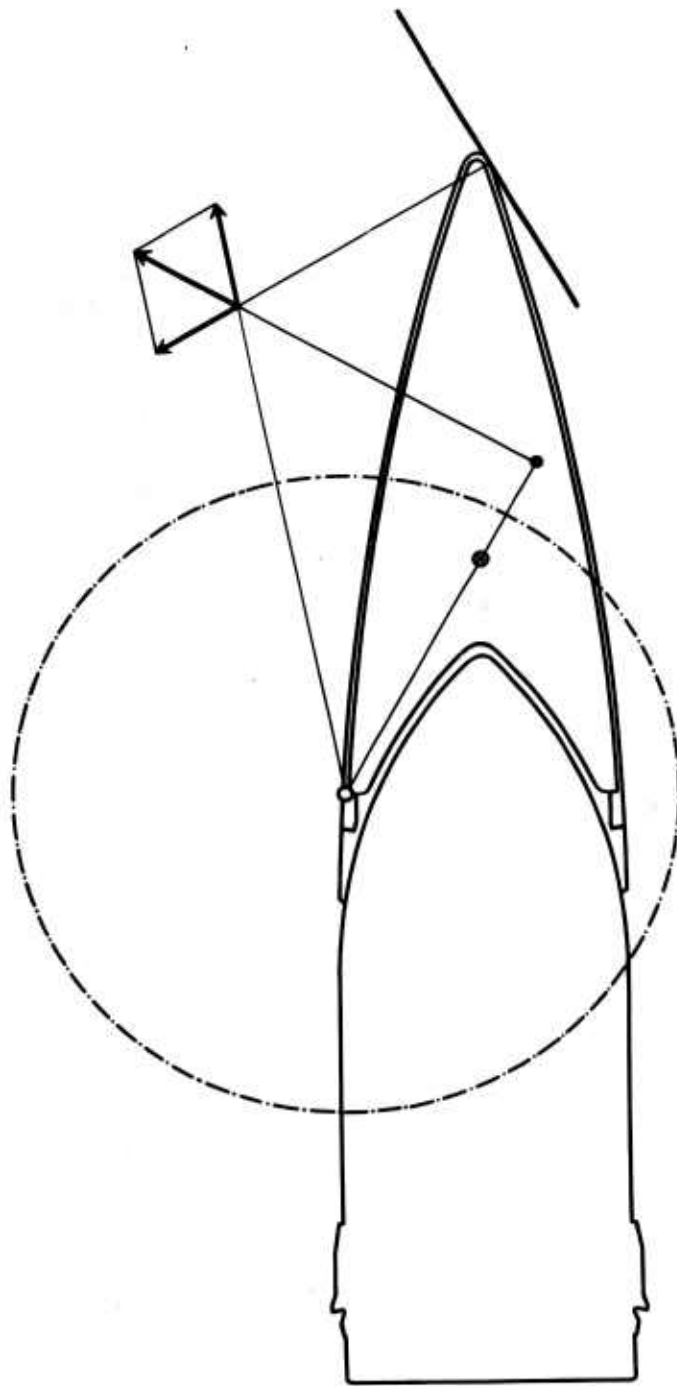


SCHEMATIC DIAGRAM TO ILLUSTRATE THE INTERACTION BETWEEN THE WINDSHIELD
AND THE HOOD WHEN THEY MOVE TOGETHER AS A SINGLE UNIT

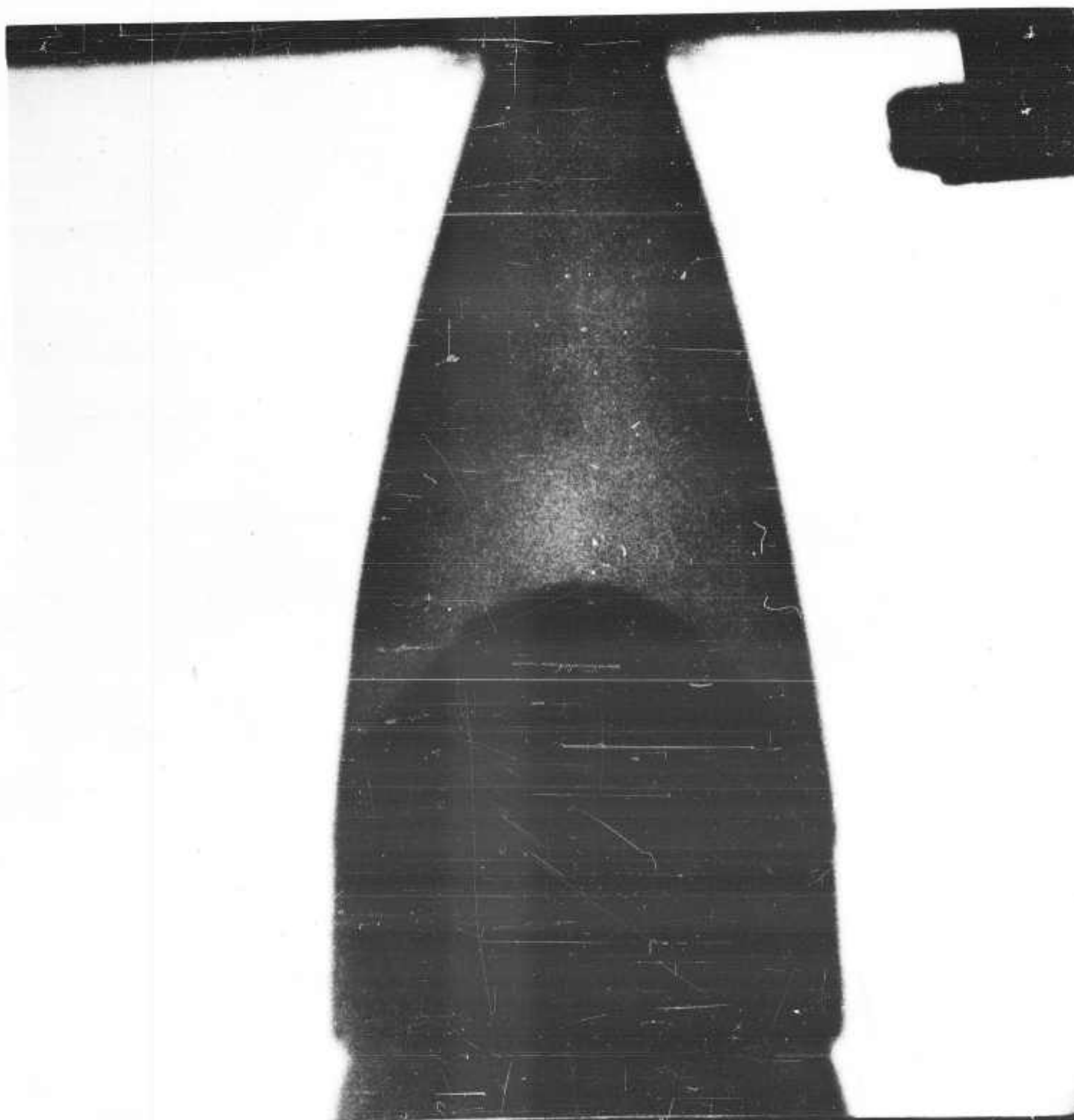
- Center of mass
- (1) refers to the windshield
- Pivot
- Center of percussion
- (2) refers to the hood

NP9 49306

FIGURE (4)



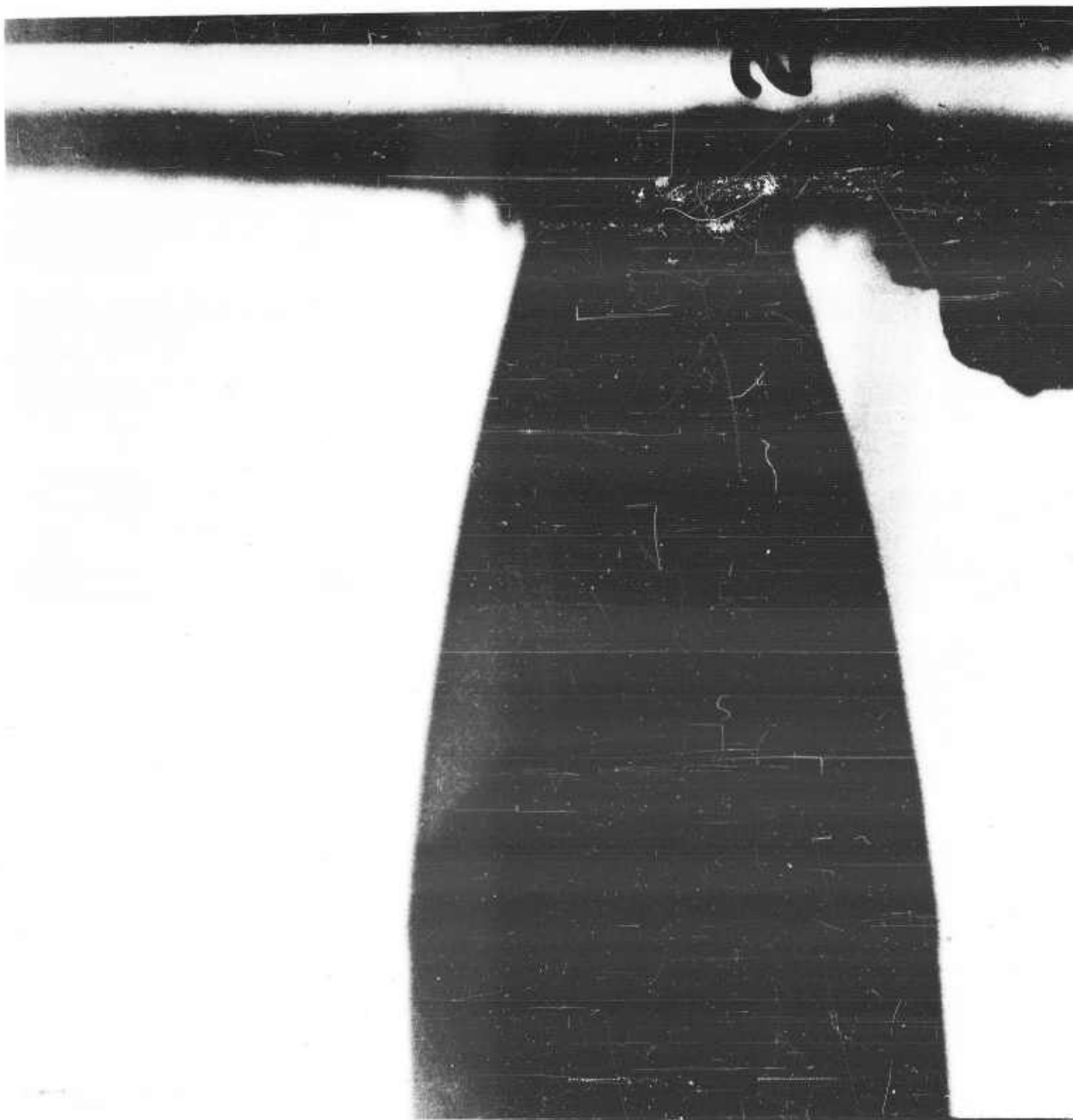
SCHEMATIC DIAGRAM TO ILLUSTRATE THE FORCES ON THE WINDSHIELD AFTER THE
THREADED RING HAS PULLED LOOSE



Flash x-radiogram of Butt Impact No. 4793 (APL). Dynamic deformation of a steel windshield.

Figure 5

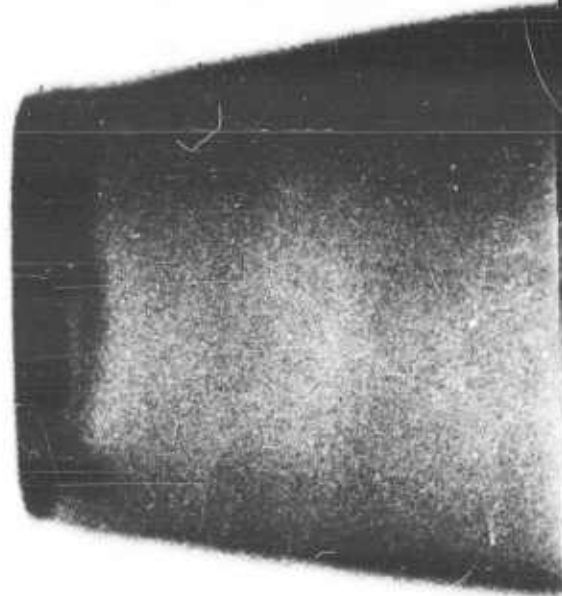
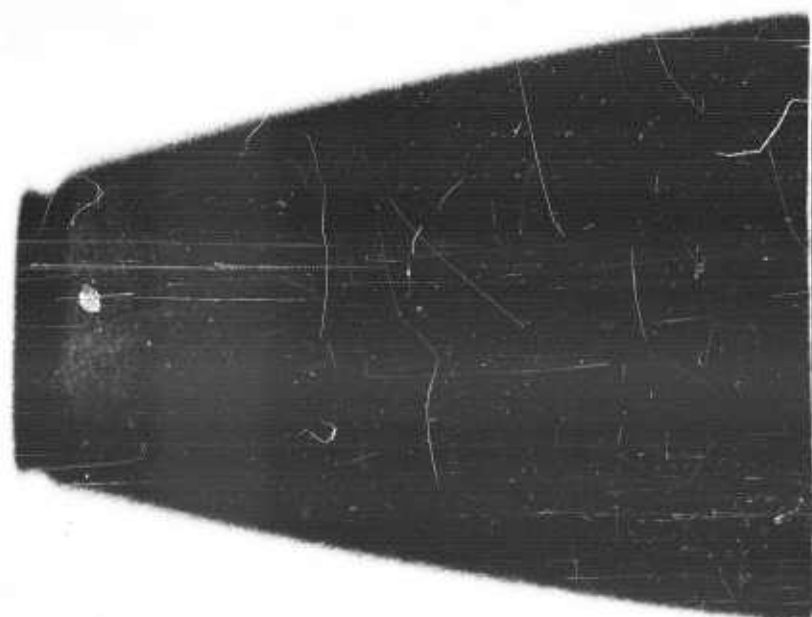
CONFIDENTIAL



Flash x-radiogram of Butt Impact No. 4798 (APL). Dynamic deformation of a steel windshield.

Figure 6

CONFIDENTIAL



CONFIDENTIAL

Flash x-radiogram of steel windshields after static compression.
Figure 7

IMP#19252

CHAR#X15463

30.68 8/35

TEST ACCEPT

Top

IMP#19251

NPG Photo No. 19942 (PPB)

CONFIDENTIAL

Bal. Accept. Test of 100# SIS Plate No. X15463 rept. Group A1031 Mfd. by Carnegie under

Cont. Nos. 82230 vs. 8" AP Mk 19-4 Proj. IL&P.

Impact Obl. S.V. (fs) 962 (Specs.)

19251 50° 1015

19252 50°

Plate passed test. May 7, 1943.

view: front - 11

Penetration 1-1/2" E 24423

Proj. rej. No thru cracks.

Comp. 24423

Thru opening 9" x 8".

Plate limit est. at 94 ± 1%.

BAL. EXPR. TEST OF 8" HP
 MK 20 PROJ. (BETH.) RWD B
 CAP VS 3-3/4" CL B. PLATE No
 GG683 AT 50 to 8/35

IMP# 15882

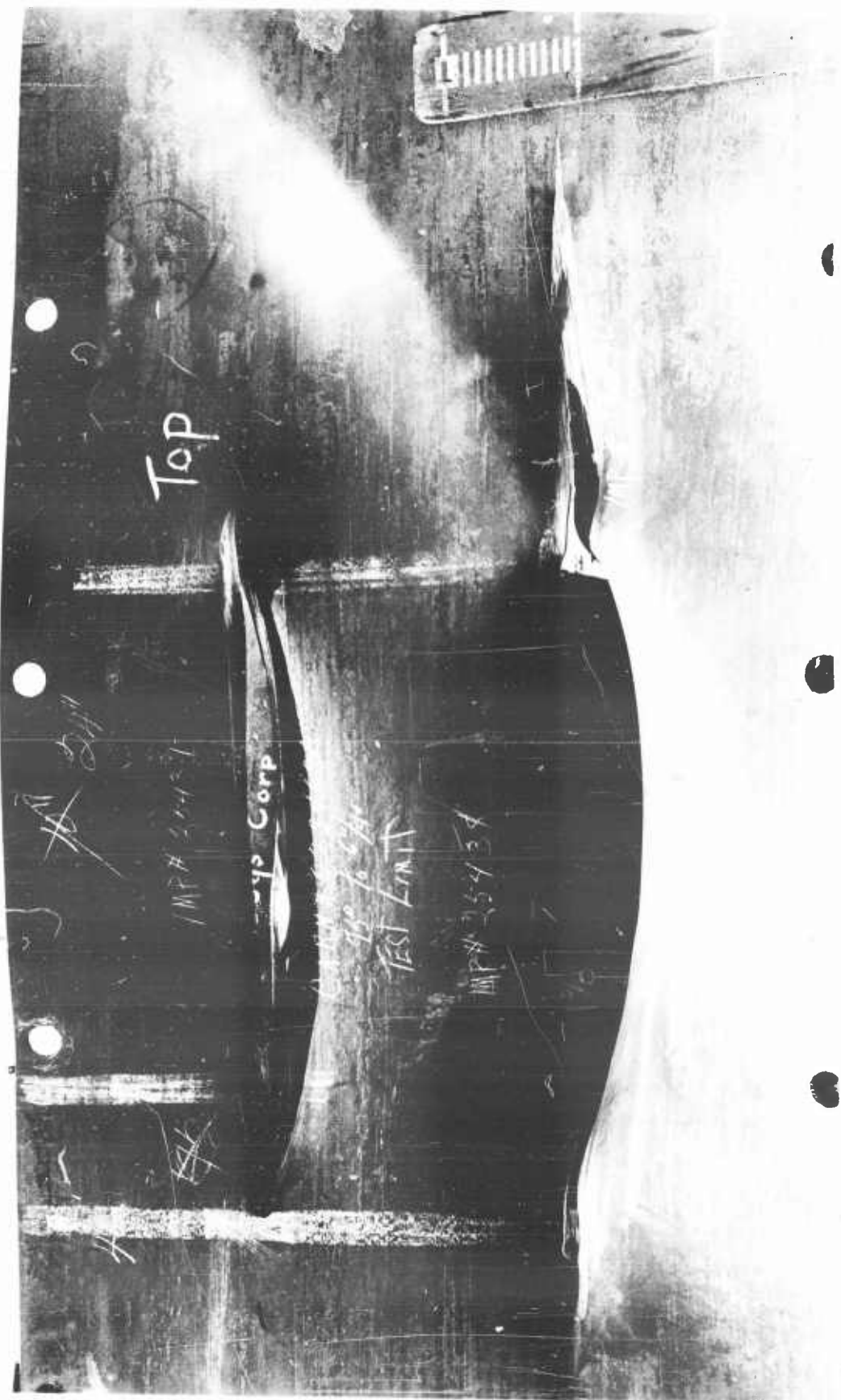
IMP# 15882

IMP# 15882
 CAP

5843

CONFIDENTIAL

NPG Photo No. 15190
 Bal. Exper. Test of 8" A.P. (260 lb.) Mk 20-4 projectile IL&P with Knobbed Cap Mfd. by
 Bethlehem under Cont. NORD 276 vs. 3-3/4" CL. B plate at ind. obl.
 S.V. (fs) VL^g Pene. Remarks
 Impact Obl. 50-15, 1603 109.2 3-1/4" Projectile rej.; not recovered; no through-crack
 15882 50-30, 1617 109.9 4-1/2" in plate.
 15883 50-30, 1617 109.9 4-1/2" Projectile rej.; eff. base slapped; 3" x 8" through crack in plate.
 View: Front of plate, side of 2nd proj. and fragments of nose caps and windshields.
 Piv



NPG Photo No. 25720 (PFB)

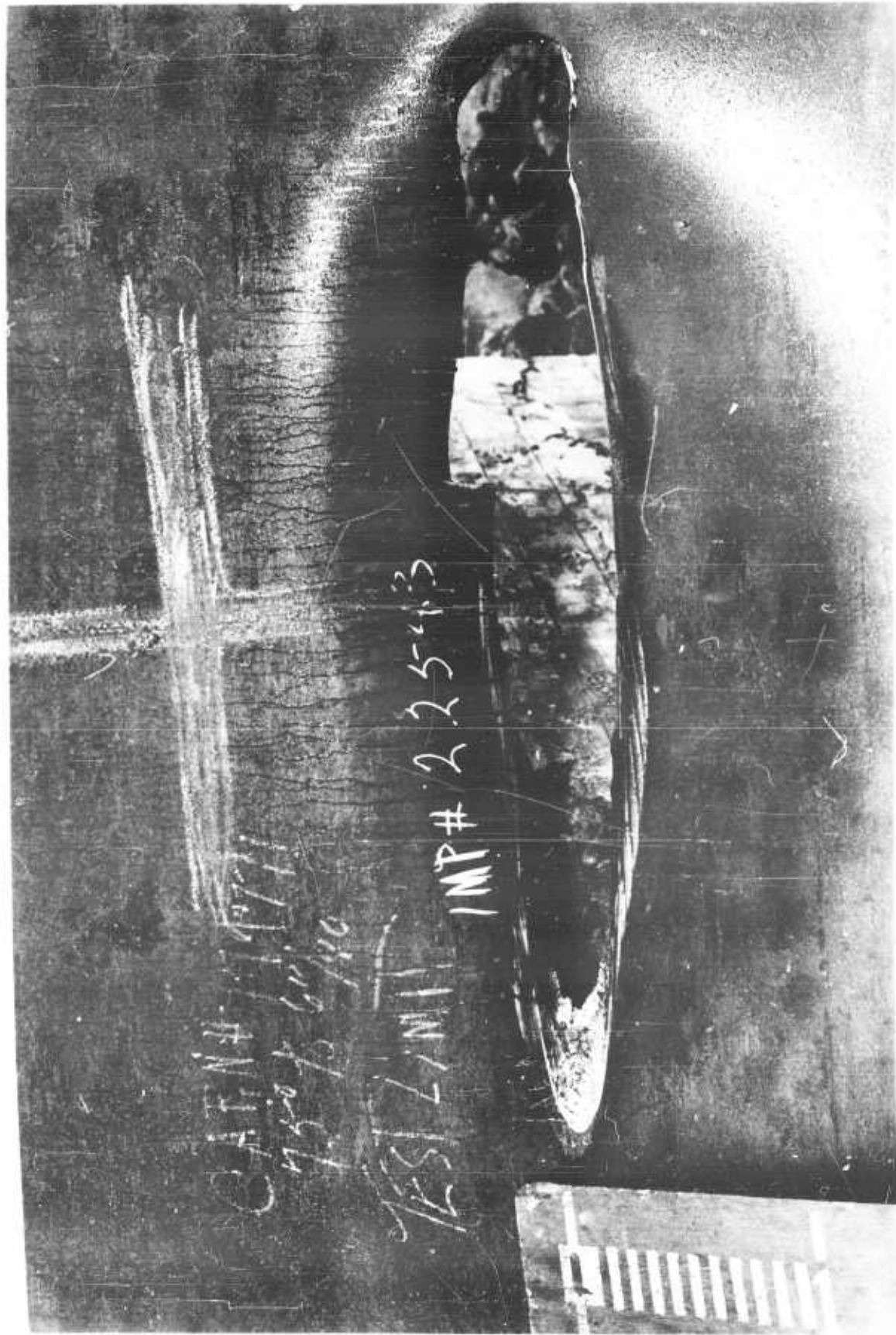
CONFIDENTIAL

Bal. Acc. Test of 20# STS Plate No. 023463A rept. group C-S26-216 Mfd. by Carn. Ill. Steel Corp. under order H-1576 vs. 6" A.P. Mk 35-4 Proj. IL&P. Plate passed test 29 May 1944.

View: Front of plate.

Impact	Obl.	S.V. (fs)	E	Pene.	% Cl. B	Thru Opening
25436	75°	797	7492	1/4"	100.4	None
25437	75°	847	7492	2"	106.8	54" x 4"
25438	75°	889	7492	3"	112.0	72" x 10-1/2"

Figure 10



NPG Photo No. 22543 (FPB)
 Ba. Acc. Fds. 504 STG Plate No. 179771 (r.p.) Setup A-1504 WFB, by Carnegie under Cont.
 3.4771 vs. 3" A.P. MK 35-1 Proj. ILSP Plate limit 8" at 102-1/2 + 16; View: front
 f plate. Plate passed test on 19 Jan 1944.
 Impact Obl. 1542
 22543
 Pene. 2" 4
 Cl. B 101.3
 Turn opening 50" 7" 8"

APPENDIX H

~~CONFIDENTIAL~~

NPG REPORT NO. 1211

DISTRIBUTION

	<u>No. of Copies</u>
Bureau of Ordnance	1
Ad3	1
Re3	1
Re3a	1
Commanding General Aberdeen Proving Ground Aberdeen, Maryland Attn: Technical Information Section Development and Proof Services	1
Commander, Operational Development Force U. S. Atlantic Fleet, U. S. Naval Base Norfolk 11, Virginia	1
Armed Services Technical Information Agency Document Service Center Knott Building Dayton 2, Ohio	5
Bureau of Ships	2
Watertown Arsenal Watertown, Massachusetts Attn: Armor Reports	1
Frankford Arsenal Philadelphia, Pennsylvania	1
Naval Ordnance Laboratory	1
Naval Ordnance Test Station Inyokern, California Attn: Rocket Reports	1
Naval Ordnance Test Station Inyokern, California Attn: Research Department	1
Naval Research Laboratory	1
Local: OK	5
OT	1
OTL	2
OKAP	1
File	1

~~CONFIDENTIAL~~

<p>MPG 1211</p> <p>Naval Proving Ground, Dahlgren, Virginia</p> <p>THE WINDSHIELD EFFECT, THE HOOD EFFECT, AND THE CAP EFFECT, by A. V. Hershby. 6 June 1955. 18p. append A-H, illus. (MPG Report No. 1211. Task Assignment E-11011-1).</p> <p>CONFIDENTIAL</p> <p>The windshield and the hood of a common projectile are demolished during the early part of an impact, and disturb the motion of the body. The force and torque on the body arise from plastic and dynamic stresses in the windshield and hood. A theory is developed for the limiting case of low velocity where the plastic stress predominates, and a theory is developed for the limiting case of high velocity where the dynamic stress predominates. The limiting theories are blended for plates of intermediate thickness by the aid of the ballistic data for common projectiles.</p>	<p>MPG 1211</p> <p>Naval Proving Ground, Dahlgren, Virginia</p> <p>THE WINDSHIELD EFFECT, THE HOOD EFFECT, AND THE CAP EFFECT, by A. V. Hershby. 6 June 1955. 18p. append A-H, illus. (MPG Report No. 1211. Task Assignment E-11011-1).</p> <p>CONFIDENTIAL</p> <p>The windshield and the hood of a common projectile are demolished during the early part of an impact, and disturb the motion of the body. The force and torque on the body arise from plastic and dynamic stresses in the windshield and hood. A theory is developed for the limiting case of low velocity where the plastic stress predominates, and a theory is developed for the limiting case of high velocity where the dynamic stress predominates. The limiting theories are blended for plates of intermediate thickness by the aid of the ballistic data for common projectiles.</p>	<p>1. Armor plate - Penetration</p> <p>2. Projectiles - Fragmentation</p> <p>I. Hershby, A. V.</p> <p>II. Title</p>	<p>1. Armor plate - Penetration</p> <p>2. Projectiles - Fragmentation</p> <p>I. Hershby, A. V.</p> <p>II. Title</p>
<p>MPG 1211</p> <p>Naval Proving Ground, Dahlgren, Virginia</p> <p>THE WINDSHIELD EFFECT, THE HOOD EFFECT, AND THE CAP EFFECT, by A. V. Hershby. 6 June 1955. 18p. append A-H, illus. (MPG Report No. 1211. Task Assignment E-11011-1).</p> <p>CONFIDENTIAL</p> <p>The windshield and the hood of a common projectile are demolished during the early part of an impact, and disturb the motion of the body. The force and torque on the body arise from plastic and dynamic stresses in the windshield and hood. A theory is developed for the limiting case of low velocity where the plastic stress predominates, and a theory is developed for the limiting case of high velocity where the dynamic stress predominates. The limiting theories are blended for plates of intermediate thickness by the aid of the ballistic data for common projectiles.</p>	<p>MPG 1211</p> <p>Naval Proving Ground, Dahlgren, Virginia</p> <p>THE WINDSHIELD EFFECT, THE HOOD EFFECT, AND THE CAP EFFECT, by A. V. Hershby. 6 June 1955. 18p. append A-H, illus. (MPG Report No. 1211. Task Assignment E-11011-1).</p> <p>CONFIDENTIAL</p> <p>The windshield and the hood of a common projectile are demolished during the early part of an impact, and disturb the motion of the body. The force and torque on the body arise from plastic and dynamic stresses in the windshield and hood. A theory is developed for the limiting case of low velocity where the plastic stress predominates, and a theory is developed for the limiting case of high velocity where the dynamic stress predominates. The limiting theories are blended for plates of intermediate thickness by the aid of the ballistic data for common projectiles.</p>	<p>1. Armor plate - Penetration</p> <p>2. Projectiles - Fragmentation</p> <p>I. Hershby, A. V.</p> <p>II. Title</p>	<p>1. Armor plate - Penetration</p> <p>2. Projectiles - Fragmentation</p> <p>I. Hershby, A. V.</p> <p>II. Title</p>

UNCLASSIFIED

UNCLASSIFIED